

國立臺灣大學醫學院腦與心智科學研究所



碩士論文

Graduate Institute of Brain and Mind Sciences

College of Medicine

National Taiwan University

Master Thesis

以神經病變痛之小鼠模式研究止痛神經迴路

Investigation of pain-relief circuits in a mouse model of  
neuropathic pain

王仁德

Jen-Te Wang

指導教授：姚皓傑 博士

Advisor: Hau-Jie Yau, Ph.D.

中華民國 108 年 8 月

August 2019

## 中文摘要



本研究旨於使用小鼠作為模式生物，研究慢性神經病變痛在大腦內的神經機轉，透過早期立即基因 *c-Fos* 的免疫染色，可以當作神經活動的生物標記，發現有神經病變痛的小鼠在前扣帶迴皮質的吻端，有較多的 *c-Fos* 表現。為了解此神經活動與神經病變痛的因果關係，本研究採用光遺傳學的方法抑制吻端前扣帶迴皮質的神經細胞活動，發現可以有效舒緩機械性輕觸痛。進一步地，本研究欲探討是否有前扣帶迴皮質相關的神經迴路負責調節此止痛效果，於是再次使用 *c-Fos* 免疫染色的方式，篩選出參與在止痛歷程中的前扣帶迴皮質傳出腦區，並挑選 *zona incerta* 及導水管周圍灰質作為兩條探討的迴路。透過光遺傳學方法抑制投射到 *zona incerta* 的前扣帶迴皮質細胞以及投射到導水管周圍灰質的前扣帶迴皮質細胞，都可以再現於前扣帶迴皮質細胞操弄所看到的行為結果，顯示這兩個下游腦區都有可能參與在前扣帶迴皮質相關的止痛歷程中。最後，為探討本研究發現對於小鼠神經病變痛的止痛效果是否具有酬賞性，光刺激自我注射模範以及制約場域偏好被用來檢驗這個問題，而發現本研究找到的所有止痛效果，都不具有酬賞性。

關鍵字:神經病變痛，光遺傳學，前扣帶迴皮質，導水管周圍灰質，光刺激自我注射模範，制約場域偏好

## Abstract

Previous human neuroimaging and rodent studies have shown that the anterior cingulate cortex (ACC) is a critical brain region in the pain matrix involved in pain processing. Accumulating evidence from rodent studies has suggested that the development of chronic pain results in synaptic reorganization of ACC. In my study, I first adopted spared nerve injury (SNI) as an animal model of neuropathic chronic pain and combined with the activity-dependent c-Fos immunostaining to identify forebrain regions involved in pain representation. After sieving out aACC as potential pain representer, I causally examined the functional roles of the aACC in neuropathic pain by using Halorhodopsin (Halo 3.0) as an inhibitory manipulation tool. I have discovered that one hour of photoinhibition can result in long-lasting relief of mechanical allodynia. To further investigate the circuits underpinnings, I employed similar c-Fos staining strategy to search for pathways mediating pain-relief in a mouse model of neuropathic pain. Finally, based on the c-Fos mapping results, I causally examined two subpopulations of aACC neurons, zona incerta-projecting aACC neurons and periaqueductal grey (PAG)-projecting aACC neurons. The results showed that photoinhibition of both circuits can alleviate mechanical allodynia. Moreover, I found that all the analgesia effects in this study were not rewarding, shown by optical intracranial self-stimulation paradigm and conditioned place preference assay. With all of the evidence, I have provided a potential clinical therapy target for resolving maladaptive symptoms of neuropathic pain without inducing addiction side effect, which is commonly accompanied by using of opioid analgesics.

Key words: neuropathic pain, optogenetics, anterior cingulate cortex, zona incerta, periaqueductal grey, conditioned place preference and optic self-administration



# Table of Contents



	Page
口試委員會審定書.....	i
中文摘要 .....	ii
Abstract.....	iii
Introduction .....	1
Chronic pain .....	1
Neuropathic pain .....	2
Human imaging study .....	3
Animal study .....	4
In this study .....	7
Results .....	9
Identification of forebrain regions involved in a mouse model of neuropathic pain .....	9
Causally examining the functional roles of the targeted brain region in neuropathic pain .....	9
Examining the modulation of neuropathic pain by chronic photoinhibition in targeted brain regions .....	11
Searching for pathways mediating pain-relief in a mouse model of neuropathic pain .....	12
Identification of brain regions involved in pain relief .....	13
Causally examining the function of the targeted neural pathways in pain relief .....	18
Examination of pain relief produced negative reinforcement .....	22
Examination of pain relief-induced reward by conventional conditioned place preference assay .....	23
Discussion .....	25
Materials and methods .....	39
References .....	47

# Introduction

## Chronic pain

According to the definition of International Association for the Study of Pain (IASP), chronic pain lasts for more than 3 months. In contrast to acute pain, it persists long time in absence of the activation of nociceptors. Accumulating evidence points out that peripheral sensitization and central sensitization in pain pathways result in chronic pain (Basbaum et al., 2009; Gold and Gebhart, 2010; Hucho and Levine, 2007; Ji et al., 2003; Luo et al., 2014; Ossipov et al., 2010; Woolf, 2011). For example, an ongoing noxious input triggers activity-dependent central sensitization in the dorsal horn of the spinal cord. In this state, spinal nociceptive neurons will have one or all of the following features: an increased excitability to noxious inputs (primary pain); an enlargement of their receptive field (secondary pain) and an ability to respond to innocuous stimuli (allodynia). The phenomenon of central sensitization shed light on the pathological explanation for various clinical chronic pain conditions no matter from the temporal, spatial or threshold change of pain sensibility perspectives (Latremoliere and Woolf, 2009; Woolf, 1983; Woolf, 2010). In the brain, sensitized neurons are also found in the thalamus and primary somatosensory cortex after partial peripheral nerve injury by using rodent model (Guilbaud et al., 1992).

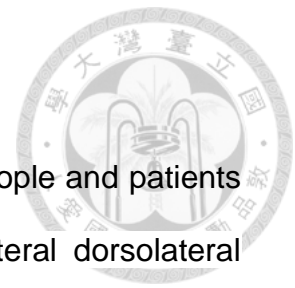
Unlike those more “event-related” brain activity such as rewarding behavior or spatial-navigation, the development of chronic pain involves longitudinal property changes in temporal dimension. However, restricted by the techniques, most of the previous studies focus on a specific time point and get a “snapshot” to

investigate. In spatial dimension, maladaptive alteration across the nociceptive pathway from spinal cord to the higher cortical regions during chronic pain state is the main question that researchers in the field are dedicated to address. In research scale, ranging from the molecular, synapses, cells, circuits to network level, different expertise are needed to provide a full comprehension of the chronic pain mechanism to help develop better therapies.

### **Neuropathic pain**

Neuropathic pain arises from a lesion or disease of the somatosensory nerve system, commonly manifesting as allodynia (pain feeling resulting from non-noxious stimulus) and hyperalgesia (heightened response from a noxious stimulus). In clinical practice, the painful symptoms and signs among patients sharing the same underlying cause usually vary (Cavaletti et al., 2011). The underlying mechanism of pain hypersensitivity and spontaneous pain in neuropathic pain are complex, and the processes remain unclear.

The prevalence of chronic neuropathic pain ranges between 6.9% and 10% of the general population (Van Hecke et al., 2014). There is a lack of solid evidence showing that neuropathic pain patients can be effectively treated by analgesics such as nonsteroidal anti-inflammatory drugs (Moore et al., 2015; Vo et al., 2009). Medicines recommended as first-line treatments such as gabapentin, pregabalin, and SSRI provide less than satisfactory relief in many patients (Finnerup et al., 2015). The evaluation and treatment for neuropathic pain require a comprehensive understanding of its neurobiological representation.



## Human imaging study

From human imaging study of comparisons between healthy people and patients with chronic back pain, gray matter density reduction in bilateral dorsolateral prefrontal cortex and right thalamus in patients has been reported (Apkarian et al., 2004). Objective spontaneous pain of chronic back pain is associated with increased activity in the medial prefrontal cortex (mPFC; including rostral anterior cingulate). In fact, mPFC activity strongly correlates with pain intensity (Baliki et al., 2006). The identified brain regions involved in spontaneous pain of postherpetic neuralgia patients are mainly located in the amygdala and ventral striatum. These regions respond most robustly to lidocaine treatment (Geha et al., 2007). fMRI study in spinal cord injury (SCI) patients demonstrates a positive correlation between persistent neuropathic pain intensity and the amount of primary somatosensory cortex (S1) reorganization (Wrigley et al., 2009). However, the concept of neural reorganization as mechanism of neuropathic pain after SCI and limb amputation is challenged by inconsistent fMRI results shown by a meta-analysis study. The opposite viewpoint has emerging evidence showing that chronic pain is associated with preserved cortical function (Jutzeler et al., 2015). Thus, different central neuropathic pain symptoms may be mediated by distinct neural mechanisms. The diversity of etiology and ectopic topography of neuropathic pain patients makes the imaging experiments difficult to gain robust statistic conclusion. Thus a consistent and controllable preclinical animal chronic pain model is needed to decipher the physiological alterations sustaining the pain



perception. Furthermore, from these non-invasive human studies, we can only get correlation results. The contrasts obtained from the experiments could be still interpreted as the consequence but not cause of chronic pain. Thus pre-clinical animal manipulation experiments will be necessary to help find the causal link between neuronal activity change and chronic pain representation.

### **Animal study**

By using rodent model as preclinical study of neuropathic pain, increased synaptic transmission in layer II and III of anterior cingulate cortex (ACC) is observed after peripheral nerve ligation (Xu et al., 2008). *In vivo* recordings in the mouse with cuffed sciatic nerve show increased firing rate and bursting activity in the ACC (Sellmeijer et al., 2018). The results from *in vivo* two-photon imaging in the ACC of spared nerve injured mice also show hyperactivity in L5 pyramidal neurons (Zhao et al., 2018). Besides the neuropathic pain model, by using *in vitro* whole-cell patch-clamp recording to investigate ACC layer II/III pyramidal neurons in inflammatory pain animal model, a reduction in the frequency of spontaneous inhibitory postsynaptic currents is observed (Koga et al., 2018). By using whole-cell recordings from ACC L5 neurons in adult mice after chronic constriction injury of the sciatic nerve, Blom et al. (2014) show that nerve injury results in potentiation of the intrinsic excitability of ACC pyramidal neurons, whereas the cellular properties of interneurons were unchanged. They further provide evidence showing that CCI causes loss of mutual connections between pyramidal neurons and fast-spiking interneurons. These structural changes suggest a potential underlying mechanism of cortical disinhibition, which may be a fundamental

pathological modification associated with peripheral nerve damage (Blom et al., 2014).

Other than ACC, different brain regions in pain pathway have distinct property changes associated with neuropathic pain. For example, during chronic pain, the medial prefrontal cortex (mPFC) is deactivated. Patch-clamp recordings reveal that cholinergic modulation of layer 5 pyramidal neurons in the mPFC is impaired one week after the nerve injury in rats. The loss of excitatory cholinergic modulation might underpin a critical role of mPFC deactivation in neuropathic pain (Radzicki et al., 2017). A local circuitry alteration in defined subpopulation of mPFC L5 neurons has been investigated in sciatic nerve CCI mice. Whole-cell recording of periaqueductal gray (PAG)-projecting mPFC neurons distinguishes a specific subregion of prelimbic but not infralimbic cortex, which has a significant reduction in excitability of retrogradely-labeled neurons contralateral to CCI side. This finding provides possible explanation for the persistence of chronic pain via disruption of descending analgesic system from the prelimbic cortex (Cheriyian and Sheets, 2018). The physiological outcomes of chronic neuropathic pain in the ACC and mPFC seem to be different, which implies their functional dissociation during pain processing.

Researchers take advantage of tools such as pharmaceuticals, optogenetic or chemogenetic tools, to attempt to reverse the alterations caused by neuropathic pain and test if it can alleviate the pain. In brain study, although it is still in its starting phase comparing to fruitful understanding of the chronic pain processing mechanism in spinal dorsal horn, there are significant findings described as the

following and the supraspinal mechanisms are receiving more and more attention nowadays. Kaang et al. have used chemogenetic tools to specifically inhibit excitatory pyramidal neurons in the ACC. They have found that it can alleviate mechanical hyperalgesia in chronic inflammatory pain model (Kang et al., 2017).

Another group has used formalin injection as animal pain model, and shown reduction of pain behavior when optogenetically stimulating inhibitory neural circuitry of the ACC (Gu et al., 2015). In pharmacology way, selective inhibitor of PKM $\zeta$  injected in the ACC can erase synaptic potentiation. It also attains the effect of normalizing pain behavior two hours after injection (Li et al., 2010).

Using a transient spinal cord ischemia model (tSCI) of neuropathic pain in mice, *in vivo* two-photon imaging and patch clamp recording show initial loss and subsequent recovery and enhancement of spontaneous firings of somatosensory cortical pyramidal neurons. Unilateral optogenetic stimulation of S1 daily after tSCI prevents and reduces pain-like behavior (Xiong et al., 2017). Moreover, chemogenetic activation of S1 somatostatin interneurons can also prevent the mechanical allodynia in SNI mice model (Cichon et al., 2017). Although mechanical allodynia induced by SNI is not affected by photoinhibition in the midcingulate division of the cingulate cortex (MCC), an activation of MCC-to-posterior insula projection is found to be sufficient to induce and maintain a hypersensitive state in the absence of peripheral noxious drive (Tan et al., 2017). Application of motor cortex stimulation in rodent model of central pain can reverse mechanical and thermal hyperalgesia, and the analgesic effect is mediated by the inhibitory nucleus zona incerta (ZI) (Lucas et al., 2011). Together, all of these

converging evidence suggests that the hyperactivity in the ACC during chronic pain plays an important role in sustaining the representation of pain perception. How to specifically manipulate those pain-modified subpopulation of neurons in the ACC without interfering with other important cognitive functions related to it will be an important research direction.

### **In this study**

Based on previous studies from human imaging in patients and electrophysiology recordings in animals of pain model, chronic pain is associated with changes in certain pain-related brain regions. Here, I hypothesize that across the development of neuropathic pain, there may be some reorganization or synaptic changes in the brain responding to the peripheral nerve injury. By comparing neural activity profile in the brain of neuropathic pain subjects to that of the control subjects, I would address those regions showing significant difference are either pain-representing or the adaptive responding to the neuropathic pain. In order to examine if these regions of interest are necessary for pain representation, I adopt optogenetic tool to photoinhibit the targeted regions and use behavioral test to observe mechanical allodynia change. Once a cortical region is identified to relieve neuropathic pain, I would further investigate which efferent regions are mediating the pain-relief effect. With the aid of retro-Cre virus combining with Cre-dependent optogenetic manipulation tool, I can attain pathway-specific manipulation to tackle this question. Through these approaches above, I have discovered a novel circuit from aACC to ZI, which is necessary for mediating mechanical allodynia but not thermal hyperalgesia. Moreover, this pain-relief effect is dissociated with reward-related

function, making it a potential clinical treatment target to avoid potential addiction issue in pain symptom control.



# Results



## Identification of forebrain regions involved in a mouse model of neuropathic pain

To identify the cortical regions involved in neuropathic chronic pain, I adopted neural activity bio-marker c-Fos staining to map neural activity pattern between SNI and Sham mice groups. On the 7th day after the surgery, I performed von Frey measurement to evaluate mechanical allodynia for confirmation of the efficacy of the SNI operation, then waited an hour to sacrifice the animal for immunohistochemistry (IHC) staining preparation. In this way, the evoked mechanical allodynia can be induced by the behavioral threshold testing, which made the c-Fos expression an event relative to a specific physiological situation. After quantitating c-Fos expressing cells in anterior part of the anterior cingulate cortex (aACC), posterior part of ACC, rostral part of the secondary motor cortex (M2), caudal M2, prelimbic cortex and infralimbic cortex, I found that c-Fos expression in the anterior part of ACC cg2 sub-region had significant enhancement in SNI group comparing to Sham group (Fig. 1A, E). No significant difference was detected in other regions that I examined. This result suggests that aACC might be critically involved in chronic neuropathic pain.

## Causally examining the functional roles of the targeted brain region in neuropathic pain

In order to examine the functional roles of the aACC's enhanced neural activity, I took advantage of optogenetic tools to examine the causal role of aACC in the

neuropathic pain. I employed Halorhodopsin (Halo 3.0) as an inhibitory manipulation tool to test whether neural activity in the aACC is required for the maintenance of neuropathic pain. For experimental design, I included three groups: experimental group which mice would receive SNI surgery then be manipulated with Halorhodopsin in the aACC, control group which mice would receive SNI surgery then be injected with eYFP reporter only to control nonspecific light elicited effect, and another control group which mice would receive Sham surgery as well as Halorhodopsin injection to control the impact of aACC silencing in pain withdrawal behavior. All three groups underwent the same one-hour continuous green light stimulation in the aACC on the 7th day after respective pain-related surgeries.

By comparing the paw withdrawal thresholds (PWT) before and after the light stimulation, the results showed that in experimental group SNI (Halo) photoinhibition in the aACC for an hour significantly resulted in an increase of the PWT, which was not found in the other two control groups (Fig. 2C). The optogenetic manipulation in the aACC did not interfere with the motor function involved in paw withdrawal since the PWT was not changed in Sham (Halo) group. This result suggests that neural activity in the aACC is required for expression of mechanical allodynia.

To test whether the pain-relief effect is transient or long-lasting, I measured the paw withdrawal threshold every 12 hours. On the selective time points of 12 hours and 24 hours after green light stimulation, the pain-relief effect from aACC photoinhibition of SNI mice still persisted. I found that by 36 hours, the withdrawal

threshold fell down to the level of SNI (eYFP) group, suggesting mechanical allodynia reinstates (Fig. 2C). The results suggest that the pain-relief by one hour photoinhibition in the aACC can sustain for at least 24 hours.

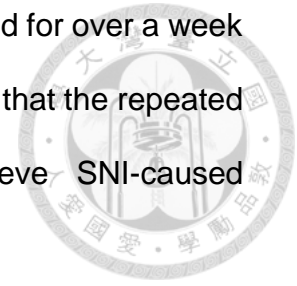
To investigate whether aACC photoinhibition can also alleviate other type of pain accompanied with SNI neuropathic pain, I further used Hargreaves test to assess thermal hyperalgesia. By using within-subject design with the same groups of animals, I found that, comparing with intact paws, SNI surgery did decrease the withdrawal latency of injured paws to heat stimulation. Interestingly, the manipulation of one hour photoinhibition in the aACC, which can alleviate mechanical allodynia, cannot alleviate the thermal hyperalgesia (Fig. 3), suggesting that aACC hyperactivity might be specifically related to mechanical allodynia but not thermal hyperalgesia.

### **Examining the modulation of neuropathic pain by chronic photoinhibition in targeted brain regions**

Due to the finding of long-lasting pain-relief effect by one hour of photoinhibition, I further examine if there is any critical period that can be interfered with to prevent the development of chronic pain. For this sake, I modified the manipulation parameter in the previous experiment, using the same one hour photoinhibition intervention but twice a day for a week immediately after the SNI/Sham surgery (Fig. 4A). Then I measured the mechanical paw withdrawal threshold at various time courses. The result demonstrated that the PWT of SNI (Halo) group did increase to the level of Sham (Halo) group right after the stimulation protocol (Fig.



4B, left panel Day7 time point), and this analgesic effect sustained for over a week since the last light stimulation. Nevertheless, the results suggest that the repeated inhibition of aACC cannot prevent and permanently relieve SNI-caused mechanical allodynia.



### **Searching for pathways mediating pain-relief in a mouse model of neuropathic pain**

Based on the above evidence, I hypothesize that the photoinhibition causes synaptic plasticity changes to maintain the long-lasting pain-relief effect. Which downstream circuits are responsible for the pain-relief effect? To tackle this question, I first set out to map the downstream regions of the aACC. By the aid of anterograde tracing of channelrhodopsin expression in the aACC, and photostimulation-induced c-Fos expression profile, I can screen candidate regions that may be directly recruited by the aACC, based on the simultaneous detection of axonal terminals—like eYFP signals and c-Fos immunolabelings. I performed c-Fos staining after photostimulating ChR2-expressing aACC to help rule out the brain regions that only showed fibers-of-passage. In this way, only those regions containing both eYFP-positive axonal terminals and enhanced c-Fos immunolabelings would be considered to be the direct downstream regions of the aACC. The results were shown in Table 1. Regions including zona incerta (ZI), periaqueductal gray (PAG), reticulotegmental nucleus of the pons (RtTg), intermediate white layer of the superior colliculus (InWh), centrolateral thalamus (CL) and claustrum (CI) show both eYFP process-like signals and enhanced c-Fos

immunolabelings. The result suggests that these regions might be directly innervated by the aACC. However, the possibility of indirect activation by aACC photostimulation via other regions cannot be ruled out in this experiment. In this case, the observed eYFP process might still be fibers-of-passage.

For those regions that show increased c-Fos expression without eYFP-positive signals, such as rostral linear nucleus, lateral habenular, paraventricular thalamic nucleus, centromedial amygdala and piriform cortex, the pattern can be interpreted as indirect recruitment by the optogenetic stimulation in the aACC. On the contrary, regions such as cerebral peduncle and ventromedial thalamus, showing axonal terminals-like eYFP signals but no enhanced c-Fos immunolabelings, are considered to be fibers-of-passage and not recruited by aACC activation.

Based on the results, I next focus the analysis of c-Fos expression between Halo and eYFP SNI mice on the following brain regions including zona incerta, periaqueductal gray, intermediate white layer of the superior colliculus, reticulotegmental nucleus of the pons, centrolateral thalamus and claustrum to examine their involvement during pain relief.

## **Identification of brain regions involved in pain relief**

### Transient intervention

To know the involvement of the aACC downstreams during one-hour photoinhibition-induced pain relief, c-Fos staining patterns were compared in three mice groups of different treatments. The group design is the same as the behavior experiments described above. There are experimental group SNI (Halo), SNI

(eYFP) group to control nonspecific light-elicited effect and Sham (Halo) to control the nonspecific effect to the pain relief by the aACC photoinhibition. I performed stereotaxic surgeries to express Halo 3.0 or eYFP in the aACC and implanted fiber optics, waited a week for animal recovery and gene expression. Then I performed SNI/Sham surgery in these mice and waited for another week for development of chronic neuropathic pain. In the 7th day after the SNI/Sham surgery, I performed von Frey test to measure the paw withdrawal threshold to make sure that mechanical allodynia was induced by SNI procedure. The green light stimulation was then applied to the aACC for an hour. I have shown that the pain-relief effect after one hour of photoinhibition in the aACC can sustain for at least 24 hours (Fig. 2C). Therefore, I chose the time point of 12 hours after the light stimulation for c-Fos staining preparation, which followed another von Frey measurement, to map involved brain regions mediating relief of mechanical allodynia.

In Figure 6, the results were from three subjects for each treatment, and each data point was obtained by averaging three slices of the comparable corresponding brain regions from the same animal. The analysis included those regions identified as aACC downstreams from Table 1. Imaging J and Photoshop were used to help quantitate the density of c-Fos-labeled cells.

I verified that the optogenetic manipulation effectively decreased the neuronal activity in the aACC because SNI (Halo) and Sham (Halo) groups show significantly decreased density of c-Fos-labeled cells in the aACC comparing to the SNI (eYFP) group (Fig. 6A). Note that there was no light application to the aACC when the von Frey measurement was performed before brain harvesting for

the c-Fos staining preparation. This result suggests that one-hour photoinhibition in the aACC is able to induce long-lasting plasticity change in the aACC, which might be the underlying mechanism of observed pain-relief effect in this study. Nevertheless, for the rest of candidate efferent regions that might be involved in pain-relief, no significant group effect was found among mice of three different treatments in terms of c-Fos immunolabeled cell density after one-way ANOVA analyses. The result implies no recruitment of these downstream regions of the aACC or the immediate early genetic tool that I adopted has insufficient sensitivity to capture the effect of one-hour photoinhibition in neuropathic pain mice.

#### Chronic intervention

In order to know whether chronic photoinhibition in the aACC can cause more dramatic synaptic plasticity changes to sustain the long-lasting pain-relief effect in the behavior results mentioned above, I adopted the same logic and procedures as the prior experiment except that the photoinhibition protocol was modified to 1-week version as the previous behavior experiment. After the SNI/Sham intervention, one-hour light stimulations were applied to the aACC twice a day with 8-hour interval for 7 consecutive days. In the 7th day I used von Frey test to measure evoked mechanical allodynia and then sacrificed the animals for c-Fos staining.

In this experiment, each group has 2 subjects. From every animal, I collected three slices of the regions that I was interested in and used the countings of six slices from two animals to perform statistics. Thus every treatment has six data points

for exploratory characterization of pain-relief profile after the aACC manipulation. I analyzed the same efferent regions as previous one hour photoinhibition experiment.



### 1.aACC

Bonferroni post hoc test after detecting group main effect among SNI (eYFP), SNI (Halo) and Sham (Halo) revealed significant differences between SNI (eYFP) vs. Sham (Halo) and SNI (Halo) vs. Sham (Halo) (Fig. 7A). The result is consistent with previous understanding of ACC's role in chronic pain. Both SNI (eYFP) and (Halo) groups had higher c-Fos immunolabeling cell densities than Sham (Halo) animal. The most behaviorally-relevant comparison that I am interested in is SNI (eYFP) vs. (Halo). Although there is no significant difference between them, a trend of lower c-Fos labeled cell density in pain-relief group (SNI with Halo) than in pain group (SNI with eYFP) can be observed in statistic summary histogram (Fig. 7A).

### 2. Claustrum (Cl)

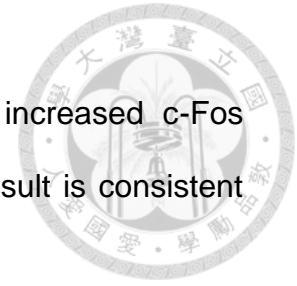
SNI (Halo) group showed significant enhancement of c-Fos expression in the claustrum comparing to the other two groups (Fig. 7B). This result suggests that these c-Fos expressing neurons in Cl of SNI Halo group might be disinhibited by the photoinhibition in the aACC.

### 3. Zona incerta (ZI)

In the pain-related region, zona incerta, SNI (Halo) group showed highest c-Fos labelings among three groups, suggesting zona incerta may be involved in pain-relief by aACC photoinhibition (Fig. 7C).

#### 4. Dorsolateral periaqueductal grey (dlPAG)

Both SNI (eYFP) and SNI (Halo) groups have significantly increased c-Fos expression comparing to Sham (Halo) group (Fig. 7D). This result is consistent with general understanding of the PAG's role in pain processing.



#### 5. Centrolateral thalamus (CL)

The pain-relief group of SNI (Halo) mice showed a significant enhancement of centrolateral thalamus c-Fos immunolabeled cell density relative to SNI (eYFP) and Sham (Halo) groups (Fig. 7E).

#### 6. Reticulotegmental nucleus of the pons

In the reticulotegmental nucleus of the pons (RtTg), there is no main effect of the treatment among the three groups in terms of c-Fos labeled cell density (Fig. 7F). The result suggests that RtTg may not be involved in the pain-relief after the aACC repeated photoinhibition.

#### 7. Intermediate white layer of the superior colliculus

In the intermediate white layer of the superior colliculus(InWh), Bonferroni post hoc test revealed a significant difference between SNI (Halo) and Sham (Halo). Although SNI (Halo) group showed significant higher c-Fos immunolabeled cell density than Sham (Halo) group, no significant difference was detected between SNI (Halo) and SNI (eYFP) group. (Fig. 7G).

#### 8. The midline of the ventral tegmental area (VTA)

Ventral tegmental area (VTA) plays a key role in reward-related behaviors. Although it is not the direct downstream of aACC based on the prior anterograde

tracing result, the relief from aversive state such as pain is considered as “negative reinforcement” or rewarding. I observed significant difference of c-Fos-expressing cell density among different conditions. The pain-relief group of SNI (Halo) had increased c-Fos immunolabeled cell density than the other two control groups, which corresponds to the notation that “pain-relief is considered as a reward”. (Fig. 7H).

### **Causally examining the function of the targeted neural pathways in pain relief**

In my study, I have shown that aACC photoinhibition relieves mechanical allodynia, and increases ZI neural activity, suggested by the c-Fos immunolabeling results. The ZI have been reported that its GABAergic neuronal activity mediates neuropathic pain in a rat sciatic nerve chronic constriction injury model (Moon and Park, 2017). Nevertheless, the role of ZI in pain or pain-relief remains unclear. Therefore, I set out to causally examine whether the aACC-to-ZI efferent output is involved in relief of neuropathic pain of SNI mice. On the other hand, although I did not found a significant difference of c-Fos expressing cell density between SNI (Halo) and SNI (eYFP) mice in the PAG, which is a well-known brain region for the role of relaying pain information, it is worth to elucidate that whether the pain-relief effect observed from aACC photoinhibition is mediated by descending pain pathway through the PAG. Therefore, the functional characterization of aACC-to-PAG efferent outputs in pain-relief was included in my study.

To attain pathway-specificity, I adopted retrograde targeting approach to employ Retro-Cre virus combining with Cre-dependent DIO-Halorhodopsin or DIO-eYFP virus to test these two circuits' roles in pain-relief (Fig. 8A). By restricted injection of retro-Cre virus in different downstream regions of the aACC, and DIO-Halorhodopsin in the aACC, cre-recombinase will be retrograde transported to all the afferent inputs of the inflected region. Only when the DIO-Halorhodopsin infected cells receive cre-recombinase can they start to express Halorhodopsin for optical manipulation. In this way, I can selectively target subpopulation of aACC neurons projecting to specific downstream regions.

To functionally examine aACC-to-ZI pathway or aACC-to-PAG pathway, I used the same one-hour photoinhibition experimental procedure as previously described. I have prepared three groups of mice, including experimental groups which aACC-to-ZI or aACC-to-PAG pathway of SNI animals were targeted and expressed with Halo 3.0 and a control group which aACC-to-ZI pathway of SNI animals were targeted and expressed with eYFP. The results showed that photoinhibition in aACC-to-ZI pathway replicated the pain-relief effect by aACC photoinhibition. The PWTs of injured paw of this group were increased by photoinhibition and were comparable to the level of control paws. This alleviation could sustain for at least 24 hours. On the other hand, inhibition of aACC-to-PAG pathway also showed partial pain-relief effect. However, the alleviation was not as effective as that of photoinhibition in aACC-to-ZI pathway although the duration of the long-lasting effect was similar (Fig. 8B).



Using continuous Halo activation to achieve inhibition in the brain may cause changes of intracellular chloride homeostasis, which might make nature synaptic GABA response excitatory after pumping in significant amount of chloride ions (Rivera et al., 1999). Thus another optogenetic inhibitory tool Arch was used to help examine this possible confounding factor. I injected DIO-Arch in the aACC combining with retro-Cre viral injection targeting ZI to specifically manipulate ZI-projecting aACC neurons (Fig. 9A). By performing the same procedure as one-hour photoinhibition as previous experiment, the result showed similar pain-relief effect as that of Halo-expressing aACC (Fig. 9). This control experiment helps us exclude the concern of GABA tone alteration by using Halorhodopsin-based inhibition.

For thermal hyperalgesia testing, none of aACC-to-ZI Halo, aACC-to-PAG Halo and aACC-to-ZI Arch groups showed increased latency of Hargreaves test after one-hour photoinhibition (Fig. 10). The group of aACC-to-ZI eYFP was served as control group for nonspecific light-elicited effect. Two-way repeated measurement ANOVA showed main effect and interaction of injury-nonjury and time course in these four groups of SNI mice. Bonferroni post hoc test was performed to analyze the response latency to thermal nociception. The results showed that in the injured operated paw, there was no significant difference before and after one-hour light stimulation in all groups of mice.

Chronic photoinhibition in aACC-to-ZI pathway prolongs the pain-relief effect over a week

In order to know whether specific manipulation of sub-population aACC neurons can attain more effective and sustained analgesia to neuropathic chronic pain, I adopted chronic therapy-like photoinhibition protocol, which is the same as that of previous experiment (Fig. 11A). The identical experimental procedure was applied to investigate the pain-relief effect by repeated photoinhibiting of aACC-to-ZI pathway. aACC-to-ZI eYFP SNI mice were prepared as control group. By measuring PWTs at various time points after the repeated light stimulations, I found that on the next day of last light stimulation, the injured paw of aACC-to-ZI Halo mice showed significant higher PWT than that of aACC-to-ZI eYFP group (Fig. 11 B left panel), suggesting relief of mechanical allodynia. Moreover, the analgesic effect sustained for more than a week and the injured paw withdrawal threshold of aACC-to-ZI Halo group decreased to comparable level as its eYFP control two weeks after last light stimulation (Fig. 11 B left panel Day 15 since SNI operation). The phenomenon was similar to the alleviation of mechanical allodynia by repeatedly silencing aACC (Fig. 4 B).

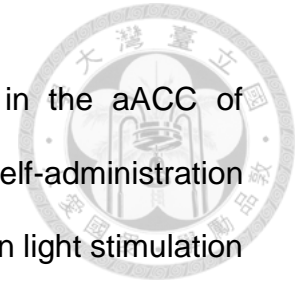
#### Identification of the cell type of ZI neurons activated by aACC photoinhibition

I would like to characterize the cell type of the c-Fos-immunolabeled cells induced by aACC photoinhibition. A double fluorescent staining with a GABAergic neuronal marker parvalbumin was performed in the SNI mice after receiving one-hour photoinhibition in the aACC. The result showed that c-Fos-positive cells and parvalbumin-positive cells in the ZI are separated populations (Fig. 12).

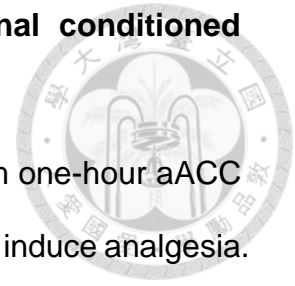
## Examination of pain relief-induced negative reinforcement

In order to know whether the pain-relief by photoinhibition in the aACC of neuropathic pain mice is rewarding, I adopted operant optic self-administration task to elucidate this question. The motivation of SNI mice to earn light stimulation in the aACC can be operationally defined and quantified by this paradigm. The assumption is that, if removal of aversive feeling such as pain serves as positive reinforcer, and aACC silencing induced pain-relief effect is selective to neuropathic pain state, then the SNI Halo mice, comparing to Sham Halo mice, are expected to show stronger motivation to press the lever to obtain photoinhibition. The two groups of mice, SNI and Sham operated mice with aACC expressing Haloehodopsin, were prepared in the experiment. Both of them were allowed to receive continuous 5s green light delivery when they pressed the active lever during 5 sessions of optic self-administration task. The results showed no significant difference in lever pressings between two groups across 5 training sessions (Fig. 13A).

Furthermore, I also performed the optic self-administration paradigm in aACC-to-ZI Halo, aACC-to-ZI eYFP and aACC-to-PAG Halo mice. All of them were subjected to SNI intervention. aACC-to-ZI Halo and aACC-to-PAG Halo mice did not show statistically significant enhancement of lever pressing across five training sessions comparing to eYFP control mice (Fig. 13B). The selective targeting of aACC efferent outputs silencing did not show rewarding effect in optical self-administration task.



## **Examination of pain relief-induced reward by conventional conditioned place preference assay**

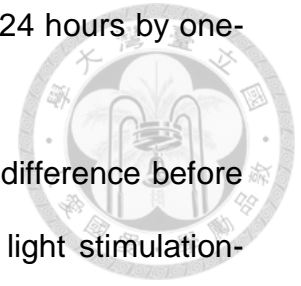


Since the observed pain-relief effect described earlier came from one-hour aACC photoinhibition, the 5s light stimulation may be not long enough to induce analgesia.

Therefore, conditioned place preference (CPP), another behavior test used for examining rewarding effect was utilized here to further examine if one-hour aACC photoinhibition elicited pain-relief can cause preference. The CPP procedure consists of three phases: a preconditioning phase of 15 minutes, a conditioning phase composed by two conditioning sessions of 30 minutes, and a preference test of 15 minutes. CPP apparatus contains two chambers distinguished by surrounding texture and connected by a central compartment. In preconditioning phase, subjects were allowed to freely access both chamber and the time spent in each zone were recorded. The preference of two chamber was served as pre-test data for analysis. On the conditioning day, animals first received one-hour of sham stimulation before being positioned to designate unpairing chamber for 30-minute conditioning. Four hours later, in the afternoon session, one-hour green light stimulation was delivered to subjects' aACC followed by conditioning in the opposite pairing chamber for 30 minute. On the third day of preference test phase, subjects were freely access to both chamber manifesting their preference or aversion of conditioned environment. The experimental design of separating light stimulation and conditioning with CPP chamber help us bypass the issue that acute optogenetic silencing of ACC might cause certain acute cognitive function disturbance related to task acquisition. Moreover, this one-trial CPP protocol is

adopted under the consideration of long-lasting pain-relief over 24 hours by one-hour aACC photoinhibition.

Both SNI (Halo) and SNI (eYFP) groups showed no significant difference before and after conditioning in terms of percentage of time spent in light stimulation-paired chamber (Fig. 14A left panel). The result suggests that one-hour photoinhibition in the aACC is not rewarding in SNI mice. Moreover, for selective aACC efferent outputs examination, aACC-to-ZI Halo and aACC-PAG Halo SNI mice also showed no significant preference for the photoinhibition-paired chamber (Fig. 14B left and right), suggesting pain-relief induced by selective inhibition of subpopulation of aACC neurons is not rewarding in one-trial CPP paradigm.



## Discussion



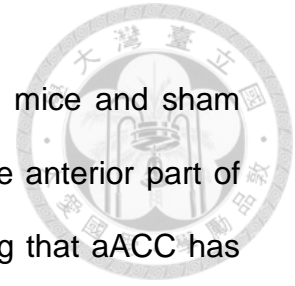
In this study I would like to explore the underlying neural mechanism of chronic neuropathic pain. By using optogenetic tool, I can causally examine the function role of pain-related regions and try to reverse the pain symptoms. Once I found targeted neuronal circuits that are involved in pain-relief, I would further validate their efficacy through various reward-related behavioral tests. To attain this aim, I first took advantage of neuronal activity biomarker, c-Fos, to capture the profile difference between chronic neuropathic pain animal model of spared nerve injury and its Sham control in various forebrain regions. The mapping revealed a contrast of higher aACC activity in SNI mice, which provided physiology-based rationale for the following causal examination via pain threshold tests. Then I confirmed that photoinhibition in the aACC can relieve mechanical allodynia caused by SNI. This result was prerequisite for further experiments of identifying possible pain-relief circuits related to the aACC. c-Fos immunolabeling were employed again to map the potential aACC downstreams involved in pain-relief. I have identified several candidate brain regions, such as zona incerta, claustrum and centrolateral thalamus. ZI and PAG were selected for further causal examination. Two pain-relief circuits of aACC-to-ZI and aACC-to-PAG were functionally characterized by using optogenetic tool in this study. In the neural circuit level, I demonstrated aACC-to-ZI and aACC-to-PAG pathways were required for maintenance of chronic neuropathic pain.

## Identifying potential neural ensembles representing pain

By using c-Fos staining comparison between neuropathic pain mice and sham surgery mice, more c-Fos-expressing cells were detected in the anterior part of ACC (aACC) of SNI group than that of Sham group, suggesting that aACC has enhanced neuronal activity in neuropathic pain state. The alteration during neuropathic pain has been observed in previous studies using intracellular-recording (Xu et al., 2008), extracellular-recording (Sellmeijer et al., 2018) and two-photon calcium imaging (Zhao et al., 2018). In other cortical regions that I have investigated, although I did not detect significant difference in terms of c-Fos immunolabeled cell density, there may still exist certain property change, such as synaptic potentiation, which cannot be revealed quantitatively by c-Fos immunostainings. Therefore, c-Fos immunoactivity can only provide us the information of which neurons are actively involved in specific event, but the information of activity level of the labeled cells is insufficient.

In addition, even when we observed comparable cell number of c-Fos-expression between SNI and Sham group, it is still possible to have induction of different populations of cells, whose activity may result in completely opposite physiological outcomes.

As an explorative experiment, c-Fos staining can provide us a quick glance of how neuronal activity state changes between different treatments in the brain. It's straightforward for us to study involved neuronal population in selective brain regions. Moreover, recently in neuroscience research field, activity-dependent targeting approaches are widely used. Among these studies, c-Fos is the most



popular-used immediate-early-gene for targeting active neuronal population. In the consideration of future direction of this study, c-Fos is a reasonable immediate early gene option to be utilized here.



## **Causal examination for candidate neural ensembles in pain representation**

### **1. Prolonged continuous photosilencing in previous pain studies**

In a previous study, researchers specifically activate inhibitory neurons in the ACC with optogenetic tool and find dramatic decrease of pain behavior during formalin test. (Gu et al., 2015). Comparing to my one-hour light stimulation, they used 45-minute light application to obtain the efficacy. In the terminals of peripheral nociceptors, photoinhibition for an hour has prolonged analgesia effect in PWT measured by von Frey test of SNI mice. Following time points of 3, 4 or 6 weeks after SNI surgery, one-hour optogenetic silencing of Na<sub>v</sub>1.8<sup>+</sup> fibers can attain pain-relief effect lasting for 3 hours. This light-elicited analgesia is completely lost until 9 weeks after SNI (Daou et al., 2016). Another study uses sciatic nerve cuffing as neuropathic pain mice model and shows that mechanical allodynia is not affected during acute optogenetic inhibition in the ACC (Sellmeijer et al., 2018). In my study, I employed one-hour continuous light stimulation to inhibit aACC of SNI mice and found it relieves mechanical allodynia for more than 24 hours.

### **2. The functional role of ACC in chronic pain**

I conducted transient and chronic photoinhibition in the aACC, and the results showed pain-relief effect in SNI mice for 24 hours and one week, respectively. This result is consistent with previous finding of the role of ACC in chronic pain. Li et al.,

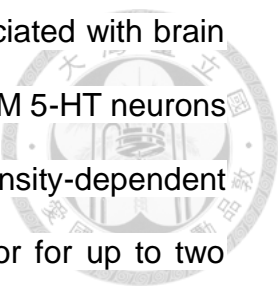


2010. perform bilaterally ACC microinjections of  $\zeta$ -pseudosubstrate inhibitory peptide (ZIP), a selective cell-permeable PKM $\zeta$  inhibitor, in mice 3 days after peripheral nerve injury. The enzyme protein kinase M zeta (PKM $\zeta$ ) maintains persistent synaptic changes and the injection of ZIP erases synaptic potentiation in the ACC, which results in significant reduction of the allodynia. The analgesic effect lasts for at least 2 hours, but wears off at 24 hours after the injection (Li et al., 2010). In this perspective, my optogenetic manipulation has more sustainable long-lasting pain-relief effect comparing to the pharmacology way, even though both cases do not specifically target sub-population of the ACC neurons.

Chemogenetic inhibition of the excitatory ACC pyramidal neurons alleviated mechanical hyperalgesia of chronic inflammatory pain model (Kang et al., 2017). Optogenetic stimulation of the inhibitory neural circuitry of the ACC also reduced pain behavior after formalin injection (Gu et al., 2015). These converging evidence demonstrated the association between reduced ACC neural activity and relief of chronic pain.

### **Mechanical allodynia and thermal hyperalgesia**

Optogenetic (SwiChR2) and chemogenetic (hM4D(Gi)) inhibition in primary afferent nociceptors enable mitigation of mechanical and thermal nociception (Iyer et al., 2016). By using CCI as a neuropathic pain mice model, optogenetic inhibition in the primary nociceptors can relieve mechanical allodynia and thermal hyperalgesia (Iyer et al., 2014). These studies suggested that different types of nociception signals can be medicated by the same “hub” before entering the brain.



The overlap of both thermal and mechanical pain behavior associated with brain activity is reported by another study. Optogenetic activation of RVM 5-HT neurons decreases both mechanical and thermal pain threshold in an intensity-dependent manner. Repeated stimulation produces sensitized pain behavior for up to two weeks (Cai et al., 2014). However, in the brain pain matrix, it remains elusive whether there is such “hub” or assemblies to be responsible for processing diverse types of nociceptive information. Mechanical allodynia, cold hyperalgesia in response to aceto and thermal hyperalgesia appear following spared nerve injury within 3 weeks (Hirai et al., 2014). Similarly, I also found that SNI mice showed significant decrease in withdrawal latency comparing to Sham mice in Hargreaves test. The assays were performed at least 3 weeks after SNI/Sham operation. Moreover, the photoinhibition in the aACC cannot relieve thermal hyperalgesia induced by SNI. Unlike inhibitory manipulation in the peripheral primary afferent nociceptors, which can tune down the sensation of both thermal and mechanical stimulus, the higher cortical region such as ACC seems specifically responsible for mechanical pain processing but not thermal pain information. The result is reasonable due to the fact that aACC is identified by c-Fos expression induced by von Frey test, which evokes mechanical allodynia. Previous study have shown that optogenetic activation of the locus ceruleus (LC) noradrenergic neurons evokes antinociceptive or pronociceptive changes in hindpaw thermal withdrawal thresholds depending on which sub-region of LC are mainly targeted (Hickey et al., 2014). If the behavior test is changed from von Frey to Hargreaves test, a different

expression profile might be acquired, which would help investigating the brain regions associated with thermal hyperalgesia.



### **Identifying pain-relief circuits from aACC photoinhibition**

I adopted both transient and chronic optogenetic manipulation in the aACC. The extent of causal alteration in the brain system might be different, but either way allows us to identify various candidate brain regions that might participate in pain-relief process by the aid of c-Fos staining mapping. By focusing on the efferent regions of the aACC, I did not find statistically significant differences among brain regions between pain and pain-relief state induced by one-hour light stimulation in the aACC. However, intense chronic photoinhibition protocol resulted in significantly higher c-Fos expression in various efferent regions of the aACC of SNI Halo mice, comparing to its eYFP control. These potential pain-relief-related regions are claustrum, centrolateral thalamus and zona incerta. Although midline of VTA did not receive axonal process from the aACC based on the ChR2 mapping experiment, I discovered a significant enhancement of c-Fos immunolabelings in this region after repeated photoinhibition in the aACC of SNI mice comparing to its Sham control and eYFP control groups. This result suggests that the pain-relief intervention might be related to the activation of rewarding system.

#### Claustrum

Claustrum has strong reciprocal connectivity with much of the cortex including the ACC and several subcortical structures (Atlan et al., 2017). The claustrum has

extensive connections linking various modality-related cortical regions of sensory and motor cortex. With this property, it has been implicated to participate in many cognitive process including directing attention (Atlan et al., 2018; Goll et al., 2015; Mathur, 2014; White et al., 2018), salience detection (Smythies et al., 2014), multisensory integration (Edelstein and Denaro, 2004), cross-modal transfer (Hadjikhani and Roland, 1998), perceptual binding (Crick and Koch, 2005), and consciousness (Koubeissi et al., 2014; Koubeissi et al., 2019; Stiefel et al., 2014). However, whether the claustrum is involved in nociception remains unknown.

### Centrolateral thalamus

There are reciprocal connection between ACC and centrolateral thalamus nucleus (CL) (Fillinger et al., 2017, 2018). I have demonstrated the aACC-to-CL projection with anterograde tracing and activity-dependent c-Fos staining. CL is involved in motor functions. It is shown by the experiment that lesion in the CL impairs performance of the rotarod test (Jeljeli et al., 2000). Projections from LC to CL are reported. Single unit recordings in LC of anaesthetized rats with simultaneous electrical stimulation in cortex or thalamus reveals that stimulation in PFC or CL produces antidromic responses in LC neurons. The study also describes electrical stimulation in LC produces a suppression of spontaneous and nociception-evoked activity in both PFC and CL cells. The employed nociceptive stimulation is noxious hot water stimulation (52°C) on the tail. With this electrophysiology evidence, it is proposed that the LC innervation could be associated with an ascending noradrenergic system acting upon a CL-PFC pain-modulation mechanism since

LC is best-known for its role of inhibiting nociceptive-evoked activity at spinal cord dorsal horn cells (Condés-Lara, 1998). Stimulation of hindlimb sensory nerve C-fibers induces expression of c-Fos in the medial thalamus including centrolateral thalamus (Pearse et al., 2001). However, the direct functional characterization evidence of CL's role in pain processing is still lacking. In my study, I found enhancement of c-Fos positive cell density in SNI Halo mice comparing to SNI eYFP mice in the CL after chronic light stimulation in the inflected aACC. The causal examination of the aACC-to-CL projection in pain-relief will be required for further investigation.

### Zona incerta

Zona incerta is a major subthalamic region which got its name standing for “zone of uncertainty”. In this decade, some of the functions in this region are described such as memory, binge-like eating and sleep (Liu et al., 2017; Zhang and van den Pol, 2017; Zhou et al., 2018). ZI GABAergic neurons also bidirectionally moderate predatory hunting (Zhao et al., 2019). Deep brain stimulation in the ZI is clinically relevant to ameliorating the symptoms of Parkinson's disease (Blomstedt et al., 2010; Khan et al., 2011; Plaha et al., 2008). The reduction of GABAergic signaling in the zona incerta is associated with the hypersensitivity in sciatic nerve chronic constriction injury (CCI) rat (Moon and Park, 2017). ZI receives widespread afferent inputs from entire cerebral cortex.

### Periaqueductal gray

Periaqueductal gray (PAG), a midbrain structure that is involved in both ascending pain transmission and descending pain modulation (Behbehani, 1995). Previous studies also have reported its role in mediating coping strategies in response to threat or stress (Assareh et al., 2016). Activating the ventrolateral PAG is associated with response involving quiescence, bradycardia, hypotension and opioid-mediated analgesia (Bandler and Shipley, 1994; Floyd et al., 2000). In contrast, excitation of the dorsolateral and lateral column induces non-opioid-mediated antinociception is accompanied with vocalization, running, jumping, hypertension and tachycardia (Depaulis and Bandler, 2012; LeDoux et al., 1988; Lewis and Gebhart, 1977; Yaksh et al., 1976).

Previous study has shown that optogenetic activation of vGluT2<sup>+</sup> vIPAG neurons has analgesic effect in tail immersion test (Tovote et al., 2016). Chemogenetic activation of glutamatergic neurons or inhibition of GABAergic neurons also suppresses thermal and mechanical hypersensitivity (Samineni et al., 2017). There is converging evidence showing that the descending pain regulation from vIPAG on the spinal nociceptive processing is through rostral ventromedial medulla (Odeh and Antal, 2001; Pertovaara et al., 1996; Waters and Lumb, 1997).

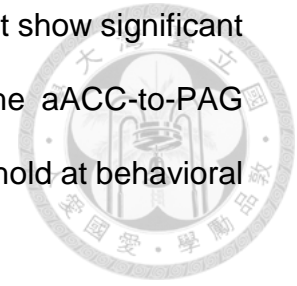
### **Causally examination of aACC-to-ZI efferent and aACC-toPAG efferent in pain-relief**

The ACC has especially abundant projection to the ZI (Mitrofanis and Mikuletic, 1999). Here, I have not only identified this connection but also characterized its involvement in neuropathic pain relief by quantitating c-Fos-expressing cells in the

ZI between ACC photoinhibition-induced pain-relief group and its respective eYFP control. Furthermore, by optogenetically targeting aACC-to-ZI efferent, I have discovered that photoinhibition of ZI-projecting ACC neurons can alleviate mechanical allodynia. Since the number of c-Fos-expressing cells in the ZI was increased following photoinhibition in the ACC, it suggests that these c-Fos-positive active neurons are possibly “disinhibited” through the microcircuit in the ZI (Fig. 15A). I have double stained these putative disinhibited c-Fos positive neurons with parvalbumin bio-marker. The result shows no colocalization between c-Fos and parvalbumin, suggesting that the ZI neurons directly innervated by the aACC may be inhibitory interneurons, which connect to the c-Fos-immunolabeled neurons activated by aACC photoinhibition. An alternative explanation for the observed phenomenon of increased c-Fos expression in the ZI induced by aACC photoinhibition is that there might be an inhibitory brain region intermediate between aACC and ZI to mediate the disinhibition (Fig. 15B). Further electrophysiology experiments will be required to examine this hypothesis.

The functional dissociation in the PAG intrigues me to further look into the mechanisms of how or whether the aACC photoinhibition-induced pain-relief is mediated by the PAG. However, I have shown that rostral ACC cg2 preferentially projects to dorsolateral PAG in anterograde tracing experiment, which is consistent with previous study that weakly labeled ACC fibers are detected in the vlPAG (Fillinger et al., 2018). The functional role of the aACC-to-dlPAG pathway in neuropathic pain-relief animal model was first elucidated. I found a partial but not complete mechanical threshold recovery after one-hour photoinhibition of this

pathway. Despite that the c-Fos mapping analysis in PAG did not show significant difference between SNI (eYFP) and SNI (Halo), I did find the aACC-to-PAG projection plays a role in mediating mechanical withdrawal threshold at behavioral level.



In the histological analysis of retrograde targeting of ZI-projecting aACC neurons, I found process-like EYFP signals in the PAG. Similarly, I also found process-like EYFP signals in the ZI from the experiment of retrograde targeting of aACC PAG-projecting neurons. The results suggest that some aACC neurons send axonal collaterals to both PAG and ZI (Fig. 15C). Given that the retrograde targeting photoinhibition was mainly applied in the aACC, I cannot rule out the possibility that the partial pain-relief effect by photoinhibition of aACC-to-PAG pathway is mediated by the aACC neurons sending axonal collaterals to ZI. The terminal manipulation of anterograde targeting of aACC-to-PAG pathway will help delineate the possible confounding of ZI involvement. Further causal examination of aACC neurons that send axonal collateral projection to ZI and PAG is also required to examine their sole contribution in chronic neuropathic pain-relief.

## **Pain-relief as a negative reward**

### Optic self-administration

In optic self-administration experiment, I did not find significant difference of lever pressing counts between Halo group and eYFP control group even though both of the subjects are under SNI-induced neuropathic pain, suggesting that lever pressing to obtain 5 s photoinhibition in the aACC is not rewarding to SNI mice.



Nevertheless, it is possible that 5s light illumination may not be enough to cause pain-relief effect. Although I have not tested if acute photoinhibition in the aACC would relieve mechanical allodynia, previous study in sciatic nerve cuffing mice shows that acute application of photoinhibition during von Frey test does not increase the paw withdrawal threshold (Sellmeijer et al., 2018).

### Conditioned place preference

In clinical situation, neuropathic chronic pain manifests simultaneously spontaneous pain and evoked pain when stimulated. However, in preclinical animal studies, the component of spontaneous pain is difficult to tackle down comparing to human study. A general way to test analgesia in spontaneous pain in animals is conditioned place preference(CPP). Analgesic agents should be rewarding only in the presence of on-going pain but not in the naive animals (King et al., 2009). For example, blocking descending facilitation by injecting lidocaine into the rostral ventromedial medulla (RVM) region of the brainstem, induces conditioned place preference in nerve-injured animals. Furthermore, when the same experiments are performed in aACC-lesion rats, those subjects showed no preference to the analgesic (Qu et al., 2011). Thus, the aACC is critical in encoding the tonic aversive state associated with chronic pain in rodents.

Lesions of the ACC can block the aversiveness of ongoing pain in both neuropathic (Barthas et al., 2015) and inflammatory pain models (Barthas et al., 2015; Chen et al., 2014; Johansen et al., 2001) In my study, I adopted one-trial conditioned place preference paradigm to examine the possible rewarding from pain-relief. Given

that aACC photoinhibition induced pain-relief can last for 24 hours, single trial but not multiple-trial CPP procedure is used to avoid the carryover of pain relief in the next conditioning session.

For conditioning phase, I separated the light stimulation and chamber-pairing to two consecutive steps instead of stimulating the aACC while the mice were posited in the conditioning chamber. The benefit of this method is that, during conditioning session, there will no possible acute cognitive dampening induced by aACC silencing. So the ability of associating the environment and event should be intact during the conditioning. With this experimental design, the result showed that SNI mice did not develop CPP to the chamber paired with pain-relieving one-hour photoinhibition in the aACC, suggesting that the optogenetic silencing of the aACC might cause sustainable plasticity in the circuits, which, mirroring the lesion study, impedes the development of CPP by pain relief.

For further evidence supporting the notation that ACC is critical in encoding aversiveness of pain, selective manipulation of excitatory neurons in the ACC can bidirectionally mediates noxious stimuli-induced conditioned place aversion (CPA). Using excitatory amino acid microinjection into the ACC of rats during conditioning produces avoidance learning in the absence of a peripheral noxious stimulus. Furthermore, microinjection of an excitatory amino acid antagonist into the ACC during conditioning blocked learning elicited by a noxious stimulus (Johansen and Fields, 2004). The later experiment result suggests that ACC activity is required for the association of pain and the environment. Although my experiment design was attempting to associate the environment with pain-relief, it's possible that

photoinhibition in the aACC can dampen the association learning. However, more refined experiment will be required to specifically address this question.



## **Conclusion**

I have a pain-relief circuit from the aACC to zona incerta. By optogenetic silencing this connection, a significant recovery of PWT in von Frey test were observed in SNI mice. The analgesic manipulation was demonstrated to be no rewarding by various behavioral paradigms. It is the significance of this property that could translate this preclinical result to clinical pain-relief application to offset against an unwanted side effect of addiction, which commonly happens in patients taking analgesics.

## Materials and Methods



**Animals.** C57BL/6J male wild-type mice (20–30 g, at least 8 weeks, NTU College of Medicine Laboratory Animal Center or National applied research laboratories) were housed in groups of 5 per cage with food and water *ad libitum* on a 12 h light/12 h dark cycle.

**Stereotaxic surgery.** 8-week-old C57BL/6J mice were deeply anaesthetized by isoflurane and fixed the position on the stereotaxic. An incision was made on the scalp and the skull was exposed. According to the coordinates of the targeted regions, corresponding holes were made with 0.4mm diameter drill bit for injections of optogenetic virus and fiber implantation. The coordinates used relative to Bregma were as follows: aACC (0.500 mm anterior,  $\pm 0.350$  mm lateral, -1.750 mm depth), ZI (1.450 mm posterior,  $\pm 0.950$  mm lateral, -4.850 mm depth), dIPAG (4.500 mm posterior,  $\pm 0.500$  mm lateral, -2.330 mm depth). For behavioral experiments, AAV virus (AAV1-Syn-eNpHR3.0-eYFP, AAV-Syn-ChR2-eYFP or AAV-Syn-eYFP from Penn Vector Core or Addgene) was injected bilaterally in the aACC. For pathway-specific behavioral experiments, Cre-dependent AAV virus (AAV-EF1 $\alpha$ -DIO-eNpHR3.0-eYFP, AAV-EF1 $\alpha$ -DIO-eYFP, AAV-EF1 $\alpha$ -DIO-Arch-eYFP from Penn Vector Core or Addgene) was injected bilaterally in the aACC and retrograde AAV virus encoding Cre recombinase (rgAAV2-Ef1a-eBFP-IRES-Cre, Addgene) was injected bilaterally in the ZI or dIPAG. 10  $\mu$ l Nanofil syringe (Hamilton, Reno, NV or World Precision Instruments, Sarasota, FL) with 33 or 34gauge needle were used to inject virus. The injections were controlled by Legato syringe pump (0.25 - 0.35  $\mu$ l, 100 nl/min) (KD scientific, Holliston, MA). For the

mice aim for optogenetic manipulations, fiber optics was implanted in the midline above the aACC (coordinates from Bregma: 0.500 mm anterior, 0.000 mm medial/lateral, -1.450 mm depth) after the injections. Dental cement and screw were used to chronic secured the fiber optics to the exposed skull. Following surgery, the mice were single housed and kept warm on a heat pad for recovery. The sites of injection and viral expression were confirmed at the end of all experiments; animals displaying incorrect expression sites were excluded from all analysis.

***Spared nerve injury (SNI) model.*** Mice were deeply anaesthetized with isoflurane, and the fur of right thigh was shaved. A 1 cm incision was made on the lateral skin surface of the thigh through the longitudinal direction distal to the knee. The muscle layer was separated by micro forcep to reveal the sciatic nerve close to the thigh bone (femur). By the aid of stereo microscope, the operator identified the area where the sural nerve branches from the sciatic nerve. The sural nerve is the smallest of the three branches. A tight surgical knot was applied around the other two branches (the tibial and common peroneal nerves). Micro scissors were used to completely severe two branches distal to the knot leaving an intact sural nerve. In sham operated animals, the sciatic nerve is exposed but not manipulated. The muscle layer was gently closed and wounds were sutured using a non-absorbable surgical suture. After the surgery, animals were left to recover in their heated home cage for several hours with easily accessible water and chow. Behavioral testing was carried out 7 d after the operation.


**Von Frey measurement.** Tactile thresholds were measured in all SNI and Sham animals at different time points post-injury. In this test, mice were placed in red colored Plexiglas boxes (9 cm length × 9 cm width × 9.5 cm height) on an elevated mesh platform. The red color of the boxes makes them unable to see each other and the operator. For each session, there were 15 min habituation before the first measurement. Mechanical threshold of hind paw withdrawal was measured by repeated manual applications of electronic von Frey filaments (Bioseb) with ascending forces to the lateral plantar surface of hind paws. The machine could gauge the force change and automatically record the value as soon as the mice withdrew their hind paws. All tests are performed on the right (injured) and left (noninjured) hind paws (5 applications per paw with 1 min inter-trial interval) separately. The average PWT was defined by excluding the maximum and minimum values out of 5 collected trials for each paw.

**Plantar test (Hargreaves' method).** To assess thermal hyperalgesia induced by SNI surgery, thermal withdrawal latency was measured using the thermal plantar test apparatus (Ugo Basile, Italy), according to the Hargreaves method. The mouse was placed individually into a red transparent acrylic box (10 cm length × 10 cm width × 14 cm height) on the elevated glass floor 12.5 cm from tabletop for 30-minute habituation. The operator located the mobile infrared heat source beneath the plantar surface of the hind paw, and started the heat-up program with automatic timer. The latency of the withdrawal response to thermal nociception was recorded by the machine. A 20 s cut-off was employed to prevent potential tissue damage in non-responsive subjects. 5 measurements were performed per hind paw (right: injured paw; left: non-injured paw) with 5 min inter-trial interval in

order to avoid accommodation or sensitization effects which might bias the results. The average thermal withdrawal latencies were calculated after excluding the maximum and minimum values out of 5 collected data points.

***Instrumental intracranial self-stimulation.*** To examine the motivation of earning photoinhibition in the aACC for pain-relief as negative reward. The behavioral experiments were conducted using SNI or Sham mice that received Halo or control vectors. After fiber implantation and gene expression, the mice underwent a habituation session of two days, exploring the standard mouse operant chambers (Panlab, Barcelona, Spain) for 40 minutes individually with optical connection. The following training session was performed for a minimum of 5-7 days. On every training day, the mice were placed into the operant chambers at the same daypart for 30 minutes (14:00-14:30). In operant chambers, mice were allowed freely access to two levers, and the active lever pressing triggered continuous 5s green laser light (532 nm, 5 mW) delivery via the implanted fiber at a fixed ratio 1 (FR1). Simultaneously, the cue light illuminated for 1 s with the house light off. On the contrary, inactive lever pressing did not result in any event in the chamber but were counted and recorded. During the 5s stimulation, additional active lever pressings were recorded but did not further trigger or prolong the laser stimulation. The behavioral experiments were performed during the mice's dark cycle.

***Conditioned place preference (CPP).*** To test the motivational drives resulting from the aversive state induced by spontaneous pain of chronic neuropathic pain, a single-trial CPP paradigm was used (King et al., 2009). This test examines whether animals develop a preference to a paired chamber due to pain relief in the



designate environment. The apparatus was positioned underneath a video camera and consisted of 3 Plexiglas chambers separated by 2 manually detachable doors. Two chambers (25.5 cm length × 13 cm width × 17 cm height) distinguished by the texture of the floor and by the wall colors (white and black), were connected by a central chamber (12 cm length × 13 cm width × 17 cm height). The CPP procedures contained three phases: a single habituation/preconditioning phase, a conditioning phase composed by two conditioning sessions of 30 minutes, and a preference test of 15 minutes. Animals went through 1 d preconditioning period during which they had access to all chambers for 15 min and acclimated to the environment. Time spent in each chamber was recorded and analyzed by Any-maze (Stoelting Co., Illinois, U.S.A.) tracking software. On the conditioning day (day 2), before entering optical-stimulation-unpaired compartment, mice first received sham light stimulation (mice were connected to laser generator's optic cable without turning on the laser power) for an hour. Four hours later, in the pairing session, mice received continuous one-hour green light stimulation (532 nm, 5 mW) in the aACC and then were placed in the opposite optical-stimulation-paired compartment. Conditioning lasted for 30 min per chamber, without allowing the animal to access the other chambers. The third day was preference test phase, during which mice were placed in the center chamber, with free access to both conditioning chambers. The time spent in each chamber was recorded for 15 min by Any-maze (Stoelting Co., Illinois, U.S.A.) tracking software and analyzed offline.

***c-Fos staining and quantification.*** Operated animals (SNI or Sham) were perfused 1 h after von Frey measurement. Coronal sections (30 μm) were collected



containing the entire regions of interest and prepared for c-Fos immunohistochemistry staining. The free-floating slices were repeatedly rinsed in PBS, permeabilized with 0.2% Triton X-100/PBS for 15 min and blocked with 3% normal goat serum (NGS) for 1 h. An overnight (16-24 h) free-floating in the mixture of rabbit anti-c-Fos antibody (1:1000 for fluorescent staining or 1:5000 for Nickel-DAB staining, ABE457, Merck Millipore) with 1% NGS, 0.2% Triton X-100 and 0.1% azide in 0.1 M PBS were subsequently performed at 4°C.

On the second day, for fluorescent staining preparation, the slices were first rinses extensively in PBS, and then incubated in PBS containing Alexa Fluor 594-conjugated goat anti-rabbit secondary antibody (1: 500, Jackson ImmunoResearch) for 1 hour at room temperature. After PB rinses, the immunostaining accomplished. The immunolabeled slices were mounted on gelatin-coated microscope slides and then cover slipped with Mowiol (Calbiochem) for visualization with a laser-scanning confocal microscope (Zeiss LSM880, Oberkochen, Germany). To obtain high resolution low-magnification images, mosaic stitching was performed with Zen software (Zeiss, Oberkochen, Germany).

If the slices were aimed for 3,3'-diaminobenzidine (DAB) staining with amplified signals by Nickel (Vector Nickel-DAB, Vector laboratories, Burlingame, California), following the overnight incubation in the primary antibody, the slices were rinsed in PBS several times on the second day. Next, operator incubated the slices with anti-rabbit IgG biotinylated secondary antibody (1:500 in PBS, Vector Laboratories) for 1 h at room temperature followed by extensive PBS washes. The slices were then incubated in PBS containing avidin-biotinylated horseradish peroxidase

complex (1:200, Elite ABC, Vector Laboratories) for 1h at room temperature. After extensive washes in PBS, c-Fos protein was visualized with Vector DAB Substrate Kit. The slices were then dehydrated and degreased for embedding in mounting medium Histokitt (Assistant, Sondheim vor der Rhön, Germany).



Nickel-DAB signals were examined and documented with a bright field light microscope (Motic RED233, Xiamen, China) equipped with CCD and integrated image processing software (SG-HD3600, SAGE Vision, Taiwan). The areas of region of interest were obtain when the images were acquired via image processing software. 3-5 sections were serially sampled from each region of interest. Image J software (version 1.52e, National Institutes of Health, USA) was used to count all c-Fos positive cells within the boundary of the defined area. A cell was considered positive only if it displayed an intensity value above the intensity threshold of the background.

**Histology.** For those optogenetically-manipulated mice, the viral expression and fiber placements were verified after all assigned experiments finished. Animals were deeply anaesthetized with isoflurane when transcardially perfused with ice-cold 0.9% saline followed by 4% paraformaldehyde (PFA) dissolved in PB. Brains were removed and stored in 4% PFA for 6h at 4 °C. After cryoprotection by 20% glycerol (wt/vol) for 16 h at 4 °C, 30-100  $\mu$ m coronal slices including the aACC, ZI and PAG were sectioned on a microtome (Leica SM 2010R, Wetzlar, Germany). Collected slices were mounted on gelatin-coated microscope slides and then cover slipped with Mowiol (Calbiochem). The placements of intracranial virus injections and optical fiber implantations were validated under fluorescence microscope.

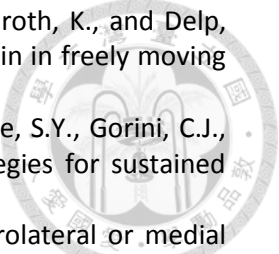
Either an insufficient bilateral viral expression in the targeted regions or a missed fiber track terminal location made the subject excluded from statistical analyses.

**Statistics.** All line charts and histograms are using mean  $\pm$  s.e.m. to represent summarized statistics results. The student's t-test and one-way ANOVA test followed by *post hoc* Bonferroni test was employed to compare data obtained from c-Fos immunolabelling experiments, conditioned place preference paradigm and behavioral thresholds as indicated in the figure legends. Two-way ANOVA for repeated measures was used in the analysis of behavioral data with time courses; *post hoc* analysis was determined using Bonferroni multiple comparisons. In all tests, the significance was determined by a value of  $P < 0.05$ . All statistical analyses were performed on Prism (GraphPad Software). The  $F_{(df1, df2)}$  or  $t$  statistical test values are reported in the legends.

## References

- Apkarian, A.V., Sosa, Y., Sonty, S., Levy, R.M., Harden, R.N., Parrish, T.B., and Gitelman, D.R. (2004). Chronic back pain is associated with decreased prefrontal and thalamic gray matter density. *Journal of neuroscience* 24, 10410-10415.
- Assareh, N., Sarraimi, M., Carrive, P., and McNally, G.P. (2016). The organization of defensive behavior elicited by optogenetic excitation of rat lateral or ventrolateral periaqueductal gray. *Behavioral neuroscience* 130, 406.
- Atlan, G., Terem, A., Peretz-Rivlin, N., Sehrawat, K., Gonzales, B.J., Pozner, G., Tasaka, G.-i., Goll, Y., Refaeli, R., and Zviran, O. (2018). The claustrum supports resilience to distraction. *Current Biology* 28, 2752-2762. e2757.
- Atlan, G., Terem, A., Peretz-Rivlin, N., Groysman, M., and Citri, A.J.J.o.C.N. (2017). Mapping synaptic cortico-claustral connectivity in the mouse. *Journal of comparative neurology* 525, 1381-1402.
- Baliki, M.N., Chialvo, D.R., Geha, P.Y., Levy, R.M., Harden, R.N., Parrish, T.B., and Apkarian, A.V. (2006). Chronic pain and the emotional brain: specific brain activity associated with spontaneous fluctuations of intensity of chronic back pain. *Journal of neuroscience* 26, 12165-12173.
- Bandler, R., and Shipley, M.T. (1994). Columnar organization in the midbrain periaqueductal gray: modules for emotional expression? *Trends in neurosciences* 17, 379-389.
- Barthas, F., Sellmeijer, J., Hugel, S., Waltisperger, E., Barrot, M., and Yalcin, I.J.B.p. (2015). The anterior cingulate cortex is a critical hub for pain-induced depression. *Biological psychiatry* 77, 236-245.
- Basbaum, A.I., Bautista, D.M., Scherrer, G., and Julius, D. (2009). Cellular and molecular mechanisms of pain. *Cell* 139, 267-284.
- Behbehani, M.M. (1995). Functional characteristics of the midbrain periaqueductal gray. *Progress in neurobiology* 46, 575-605.
- Blom, S.M., Pfister, J.-P., Santello, M., Senn, W., and Nevian, T. (2014). Nerve injury-induced neuropathic pain causes disinhibition of the anterior cingulate cortex. *Journal of neuroscience* 34, 5754-5764.
- Blomstedt, P., Sandvik, U., and Tisch, S. (2010). Deep brain stimulation in the posterior subthalamic area in the treatment of essential tremor. *Movement disorders* 25, 1350-1356.
- Cai, Y.-Q., Wang, W., Hou, Y.-Y., and Pan, Z.Z. (2014). Optogenetic activation of brainstem serotonergic neurons induces persistent pain sensitization. *Molecular pain* 10, 70.
- Cavaletti, G., Alberti, P., Frigeni, B., Piatti, M., and Susani, E. (2011). Chemotherapy-induced neuropathy. *Current treatment options in neurology* 13, 180-190.
- Chen, T., Koga, K., Descalzi, G., Qiu, S., Wang, J., Zhang, L.-S., Zhang, Z.-J., He, X.-B., Qin, X., and Xu, F.-Q. (2014). Postsynaptic potentiation of corticospinal projecting neurons in the anterior cingulate cortex after nerve injury. *Molecular pain* 10, 33.
- Cheriyian, J., and Sheets, P.L. (2018). Altered excitability and local connectivity of mPFC-PAG neurons in a mouse model of neuropathic pain. *Journal of neuroscience* 38, 4829-4839.
- Cichon, J., Blanck, T.J., Gan, W.-B., and Yang, G. (2017). Activation of cortical somatostatin interneurons prevents the development of neuropathic pain. *Nature neuroscience* 20, 1122.
- Condés-Lara, M. (1998). Different direct pathways of locus coeruleus to medial prefrontal cortex and centrolateral thalamic nucleus: electrical stimulation effects on the evoked responses to nociceptive peripheral stimulation. *European journal of pain* 2, 15-23.

- Crick, F.C., and Koch, C. (2005). What is the function of the claustrum? *Philosophical transactions of the royal society b biological sciences* 360, 1271-1279.
- Daou, I., Beaudry, H., Ase, A.R., Wieskopf, J.S., Ribeiro-da-Silva, A., Mogil, J.S., and Séguéla, P. (2016). Optogenetic silencing of Nav1. 8-positive afferents alleviates inflammatory and neuropathic pain. *eNeuro* 3.
- Depaulis, A., and Bandler, R. (2012). The midbrain periaqueductal gray matter: Functional, anatomical, and neurochemical organization, Vol 213 (Springer Science & Business Media).
- Edelstein, L., and Denaro, F. (2004). The claustrum: a historical review of its anatomy, physiology, cytochemistry and functional significance. *Cellular and molecular biology* 104, 368,415,434,556,557.
- Fillinger, C., Yalcin, I., Barrot, M., and Veinante, P. (2017). Afferents to anterior cingulate areas 24a and 24b and midcingulate areas 24a' and 24b' in the mouse. *Brain Structure and Function* 222, 1509-1532.
- Fillinger, C., Yalcin, I., Barrot, M., and Veinante, P. (2018). Efferents of anterior cingulate areas 24a and 24b and midcingulate areas 24a' and 24b' in the mouse. *Brain structure and function* 223, 1747-1778.
- Finnerup, N.B., Attal, N., Haroutounian, S., McNicol, E., Baron, R., Dworkin, R.H., Gilron, I., Haanpää, M., Hansson, P., and Jensen, T.S. (2015). Pharmacotherapy for neuropathic pain in adults: a systematic review and meta-analysis. *The lancet neurology* 14, 162-173.
- Floyd, N.S., Price, J.L., Ferry, A.T., Keay, K.A., and Bandler, R. (2000). Orbitomedial prefrontal cortical projections to distinct longitudinal columns of the periaqueductal gray in the rat. *Journal of comparative neurology* 422, 556-578.
- Geha, P., Baliki, M.N., Chialvo, D., Harden, R.N., Paice, J., and Apkarian, A. (2007). Brain activity for spontaneous pain of postherpetic neuralgia and its modulation by lidocaine patch therapy. *Pain* 128, 88-100.
- Gold, M.S., and Gebhart, G.F. (2010). Nociceptor sensitization in pain pathogenesis. *Nature medicine* 16, 1248.
- Goll, Y., Atlan, G., and Citri, A. (2015). Attention: the claustrum. *Trends in neurosciences* 38, 486-495.
- Gu, L., Uhelski, M.L., Anand, S., Romero-Ortega, M., Kim, Y.-t., Fuchs, P.N., and Mohanty, S.K. (2015). Pain inhibition by optogenetic activation of specific anterior cingulate cortical neurons. *PLoS one* 10, e0117746.
- Guilbaud, G., Benoist, J., Levante, A., Gautron, M., and Willer, J. (1992). Primary somatosensory cortex in rats with pain-related behaviours due to a peripheral mononeuropathy after moderate ligation of one sciatic nerve: neuronal responsivity to somatic stimulation. *Experimental brain* 92, 227-245.
- Hadjikhani, N., and Roland, P.E. (1998). Cross-modal transfer of information between the tactile and the visual representations in the human brain: a positron emission tomographic study. *Journal of neuroscience* 18, 1072-1084.
- Hickey, L., Li, Y., Fyson, S.J., Watson, T.C., Perrins, R., Hewinson, J., Teschemacher, A.G., Furue, H., Lumb, B.M., and Pickering, A.E. (2014). Optoactivation of locus ceruleus neurons evokes bidirectional changes in thermal nociception in rats. *Journal of neuroscience* 34, 4148-4160.
- Hirai, T., Enomoto, M., Kaburagi, H., Sotome, S., Yoshida-Tanaka, K., Ukegawa, M., Kuwahara, H., Yamamoto, M., Tajiri, M., and Miyata, H. (2014). Intrathecal AAV serotype 9-mediated delivery of shRNA against TRPV1 attenuates thermal hyperalgesia in a mouse model of peripheral nerve injury. *Molecular therapy* 22, 409-419.
- Hucho, T., and Levine, J.D. (2007). Signaling pathways in sensitization: toward a nociceptor cell biology. *Neuron* 55, 365-376.



Iyer, S.M., Montgomery, K.L., Towne, C., Lee, S.Y., Ramakrishnan, C., Deisseroth, K., and Delp, S.L.J.N.b. (2014). Virally mediated optogenetic excitation and inhibition of pain in freely moving nontransgenic mice. *Nature biotechnology* 32, 274.

Iyer, S.M., Vesuna, S., Ramakrishnan, C., Huynh, K., Young, S., Berndt, A., Lee, S.Y., Gorini, C.J., Deisseroth, K., and Delp, S.L. (2016). Optogenetic and chemogenetic strategies for sustained inhibition of pain. *Scientific reports* 6, 30570.

Jeljeli, M., Strazielle, C., Caston, J., and Lalonde, R. (2000). Effects of centrolateral or medial thalamic lesions on motor coordination and spatial orientation in rats. *Neuroscience research* 38, 155-164.

Ji, R.-R., Kohno, T., Moore, K.A., and Woolf, C.J. (2003). Central sensitization and LTP: do pain and memory share similar mechanisms? *Trends in neurosciences* 26, 696-705.

Johansen, J.P., and Fields, H.L. (2004). Glutamatergic activation of anterior cingulate cortex produces an aversive teaching signal. *Nature neuroscience* 7, 398.

Johansen, J.P., Fields, H.L., and Manning, B.H. (2001). The affective component of pain in rodents: direct evidence for a contribution of the anterior cingulate cortex. *PNAS* 98, 8077-8082.

Jutzeler, C., Curt, A., and Kramer, J. (2015). Relationship between chronic pain and brain reorganization after deafferentation: a systematic review of functional MRI findings. *NeuroImage: Clinical* 9, 599-606.

Kang, S.J., Kim, S., Lee, J., Kwak, C., Lee, K., Zhuo, M., and Kaang, B.-K. (2017). Inhibition of anterior cingulate cortex excitatory neuronal activity induces conditioned place preference in a mouse model of chronic inflammatory pain. *The Korean Journal of Physiology & Pharmacology* 21, 487-493.

Khan, S., Mooney, L., Plaha, P., Javed, S., White, P., Whone, A.L., and Gill, S.S. (2011). Outcomes from stimulation of the caudal zona incerta and pedunculopontine nucleus in patients with Parkinson's disease. *British journal of neurosurgery* 25, 273-280.

King, T., Vera-Portocarrero, L., Gutierrez, T., Vanderah, T.W., Dussor, G., Lai, J., Fields, H.L., and Porreca, F. (2009). Unmasking the tonic-aversive state in neuropathic pain. *Nature neuroscience* 12, 1364.

Koga, K., Shimoyama, S., Yamada, A., Furukawa, T., Nikaido, Y., Furue, H., Nakamura, K., and Ueno, S. (2018). Chronic inflammatory pain induced GABAergic synaptic plasticity in the adult mouse anterior cingulate cortex. *Molecular pain* 14, 1744806918783478.

Koubeissi, M.Z., Bartolomei, F., Beltagy, A., and Picard, F. (2014). Electrical stimulation of a small brain area reversibly disrupts consciousness. *Epilepsy & behavior* 37, 32-35.

Koubeissi, M.Z., Kurada, L., Bayat, A., and Joshi, S. (2019). The Claustrum in Relation to Seizures and Electrical Stimulation. *Frontiers in neuroanatomy* 13, 8.

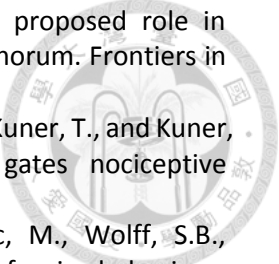
Latremoliere, A., and Woolf, C.J. (2009). Central sensitization: a generator of pain hypersensitivity by central neural plasticity. *The journal of pain* 10, 895-926.

LeDoux, J.E., Iwata, J., Cicchetti, P., and Reis, D.J. (1988). Different projections of the central amygdaloid nucleus mediate autonomic and behavioral correlates of conditioned fear. *Journal of neuroscience* 8, 2517-2529.

Lewis, V.A., and Gebhart, G. (1977). Evaluation of the periaqueductal central gray (PAG) as a morphine-specific locus of action and examination of morphine-induced and stimulation-produced analgesia at coincident PAG loci. *Brain research* 124, 283-303.

Li, X.-Y., Ko, H.-G., Chen, T., Descalzi, G., Koga, K., Wang, H., Kim, S.S., Shang, Y., Kwak, C., and Park, S.-W. (2010). Alleviating neuropathic pain hypersensitivity by inhibiting PKM $\zeta$  in the anterior cingulate cortex. *Science* 330, 1400-1404.

- Liu, K., Kim, J., Kim, D.W., Zhang, Y.S., Bao, H., Denaxa, M., Lim, S.-A., Kim, E., Liu, C., and Wickersham, I. (2017). Lhx6-positive GABA-releasing neurons of the zona incerta promote sleep. *Nature* 548, 582.
- Lucas, J.M., Ji, Y., and Masri, R. (2011). Motor cortex stimulation reduces hyperalgesia in an animal model of central pain. *Pain* 152, 1398-1407.
- Luo, C., Kuner, T., and Kuner, R. (2014). Synaptic plasticity in pathological pain. *Trends in neurosciences* 37, 343-355.
- Mathur, B.N. (2014). The claustrum in review. *Frontiers in systems neuroscience* 8, 48.
- Mitrofanis, J., and Mikuletic, L. (1999). Organisation of the cortical projection to the zona incerta of the thalamus. *Journal of comparative neurology* 412, 173-185.
- Moon, H.C., and Park, Y.S. (2017). Reduced GABAergic neuronal activity in zona incerta causes neuropathic pain in a rat sciatic nerve chronic constriction injury model. *Journal of pain research* 10, 1125.
- Moore, R.A., Chi, C.C., Wiffen, P.J., Derry, S., and Rice, A.S. (2015). Oral nonsteroidal anti-inflammatory drugs for neuropathic pain. *Cochrane database of systematic reviews*.
- Odeh, F., and Antal, M. (2001). The projections of the midbrain periaqueductal grey to the pons and medulla oblongata in rats. *European journal of neuroscience* 14, 1275-1286.
- Ossipov, M.H., Dussor, G.O., and Porreca, F. (2010). Central modulation of pain. *The journal of clinical investigation* 120, 3779-3787.
- Paxinos, G., and Franklin, K.B. (2019). Paxinos and Franklin's the mouse brain in stereotaxic coordinates (Academic press).
- Pearse, D.D., Bushell, G., and Leah, J. (2001). Jun, Fos and Krox in the thalamus after C-fiber stimulation: coincident-input-dependent expression, expression across somatotopic boundaries, and nucleolar translocation. *Journal of neuroscience* 107, 143-159.
- Pertovaara, A., Wei, H., and Härmäläinen, M.M. (1996). Lidocaine in the rostroventromedial medulla and the periaqueductal gray attenuates allodynia in neuropathic rats. *Neuroscience letters* 218, 127-130.
- Plaha, P., Khan, S., and Gill, S.S. (2008). Bilateral stimulation of the caudal zona incerta nucleus for tremor control. *Journal of neurology, neurosurgery & psychiatry* 79, 504-513.
- Qu, C., King, T., Okun, A., Lai, J., Fields, H.L., and Porreca, F. (2011). Lesion of the rostral anterior cingulate cortex eliminates the aversiveness of spontaneous neuropathic pain following partial or complete axotomy. *Pain* 152, 1641-1648.
- Radzicki, D., Pollema-Mays, S.L., Sanz-Clemente, A., and Martina, M. (2017). Loss of M1 receptor dependent cholinergic excitation contributes to mPFC deactivation in neuropathic pain. *Journal of neuroscience* 37, 2292-2304.
- Rivera, C., Voipio, J., Payne, J.A., Ruusuvuori, E., Lahtinen, H., Lamsa, K., Pirvola, U., Saarma, M., and Kaila, K. (1999). The K<sup>+</sup>/Cl<sup>-</sup> co-transporter KCC2 renders GABA hyperpolarizing during neuronal maturation. *Nature* 397, 251.
- Samineni, V.K., Grajales-Reyes, J.G., Copits, B.A., O'Brien, D.E., Trigg, S.L., Gomez, A.M., Bruchas, M.R., and Gereau IV, R.W. (2017). Divergent modulation of nociception by glutamatergic and GABAergic neuronal subpopulations in the periaqueductal gray. *eNeuro* 4.
- Sellmeijer, J., Mathis, V., Hugel, S., Li, X.-H., Song, Q., Chen, Q.-Y., Barthas, F., Lutz, P.-E., Karatas, M., and Luthi, A. (2018). Hyperactivity of anterior cingulate cortex areas 24a/24b drives chronic pain-induced anxiodepressive-like consequences. *Journal of neuroscience* 38, 3102-3115.
- Smythies, J., Edelstein, L., and Ramachandran, V. (2014). Hypotheses relating to the function of the claustrum II: does the claustrum use frequency codes? *Frontiers in integrative neuroscience* 8, 7.



Stiefel, K.M., Merrifield, A., and Holcombe, A.O. (2014). The claustrum's proposed role in consciousness is supported by the effect and target localization of *Salvia divinorum*. *Frontiers in integrative neuroscience* 8, 20.

Tan, L.L., Pelzer, P., Heintz, C., Tang, W., Gangadharan, V., Flor, H., Sprengel, R., Kuner, T., and Kuner, R. (2017). A pathway from midcingulate cortex to posterior insula gates nociceptive hypersensitivity. *Nature neuroscience* 20, 1591.

Tovote, P., Esposito, M.S., Botta, P., Chaudun, F., Fadok, J.P., Markovic, M., Wolff, S.B., Ramakrishnan, C., Fenno, L., and Deisseroth, K. (2016). Midbrain circuits for defensive behaviour. *Nature* 534, 206.

Van Hecke, O., Austin, S.K., Khan, R.A., Smith, B., and Torrance, N. (2014). Neuropathic pain in the general population: a systematic review of epidemiological studies. *PAIN* 155, 654-662.

Vo, T., Rice, A.S., and Dworkin, R.H. (2009). Non-steroidal anti-inflammatory drugs for neuropathic pain: how do we explain continued widespread use? *Pain* 143, 169-171.

Waters, A., and Lumb, B. (1997). Inhibitory effects evoked from both the lateral and ventrolateral periaqueductal grey are selective for the nociceptive responses of rat dorsal horn neurones. *Brain research* 752, 239-249.

White, M.G., Panicker, M., Mu, C., Carter, A.M., Roberts, B.M., Dharmasri, P.A., and Mathur, B.N. (2018). Anterior cingulate cortex input to the claustrum is required for top-down action control. *Cell reports* 22, 84-95.

Woolf, C.J. (1983). Evidence for a central component of post-injury pain hypersensitivity. *Nature* 306, 686.

Woolf, C.J. (2010). What is this thing called pain? *The Journal of clinical investigation* 120, 3742-3744.

Woolf, C.J. (2011). Central sensitization: implications for the diagnosis and treatment of pain. *Pain* 152, S2-S15.

Wrigley, P.J., Press, S.R., Gustin, S.M., Macefield, V.G., Gandevia, S.C., Cousins, M.J., Middleton, J.W., Henderson, L.A., and Siddall, P. (2009). Neuropathic pain and primary somatosensory cortex reorganization following spinal cord injury. *Pain* 141, 52-59.

Xiong, W., Ping, X., Ripsch, M.S., Chavez, G.S.C., Hannon, H.E., Jiang, K., Bao, C., Jadhav, V., Chen, L., and Chai, Z. (2017). Enhancing excitatory activity of somatosensory cortex alleviates neuropathic pain through regulating homeostatic plasticity. *Scientific reports* 7, 12743.

Xu, H., Wu, L.-J., Wang, H., Zhang, X., Vadakkan, K.I., Kim, S.S., Steenland, H.W., and Zhuo, M. (2008). Presynaptic and postsynaptic amplifications of neuropathic pain in the anterior cingulate cortex. *Journal of neuroscience* 28, 7445-7453.

Yaksh, T.L., Yeung, J.C., and Rudy, T.A. (1976). Systematic examination in the rat of brain sites sensitive to the direct application of morphine: observation of differential effects within the periaqueductal gray. *Brain research* 114, 83-103.

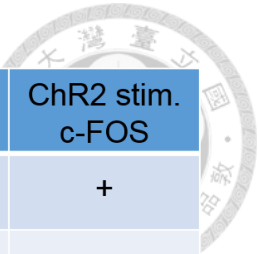
Zhang, X., and van den Pol, A.N. (2017). Rapid binge-like eating and body weight gain driven by zona incerta GABA neuron activation. *Science* 356, 853-859.

Zhao, R., Zhou, H., Huang, L., Xie, Z., Wang, J., Gan, W.-B., and Yang, G. (2018). Neuropathic pain causes pyramidal neuronal hyperactivity in the anterior cingulate cortex. *Frontiers in cellular neuroscience* 12, 107.

Zhao, Z.-d., Chen, Z., Xiang, X., Hu, M., Xie, H., Jia, X., Cai, F., Cui, Y., Chen, Z., and Qian, L. (2019). Zona incerta GABAergic neurons integrate prey-related sensory signals and induce an appetitive drive to promote hunting. *Nature neuroscience* 22, 921.

Zhou, M., Liu, Z., Melin, M.D., Ng, Y.H., Xu, W., and Südhof, T. (2018). A central amygdala to zona incerta projection is required for acquisition and remote recall of conditioned fear memory. *Nature neuroscience* 21, 1515.





	eYFP process	ChR2 stim. c-FOS		eYFP process	ChR2 stim. c-FOS
zona incerta	+	+	Centrolateral thalamus	+	+
Periaqueductal gray	+	+	Clastrum	+	+
Reticulotegmen- tal nucleus of the pons	+	+	Lateral septal nucleus	-	+
Rostral linear nucleus	-	+	Centromedial amygdala	-	+
Cerebral peduncle	+	-	Basolateral amygdala	-	+
Intermediate white layer of the superior colliculus	+	+	Piriform cortex	-	+
Lateral habenular	-	+	Ventromedial thalamus	+	-
Paraventricular thalamic nucleus	-	+			

Table 1. Mapping of possible aACC efferent brain regions and their functional recruitments by using channelrhodopsin and c-Fos immunostaining. “+” denotes detected signals; “-” denotes no detectable signals.

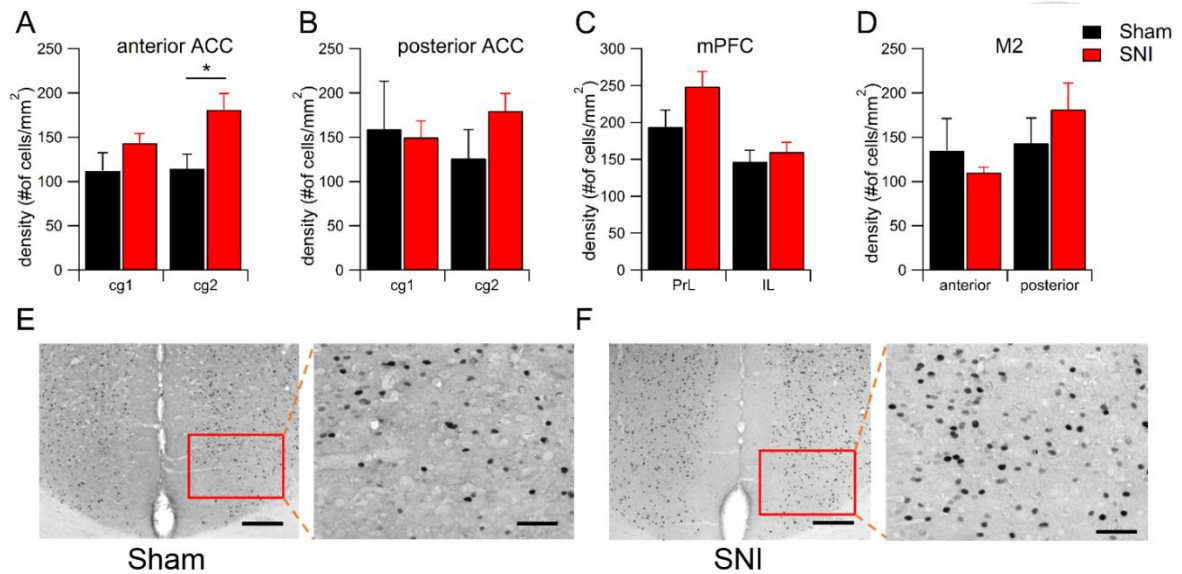


Figure 1. c-Fos immunolabeling experiment of SNI versus Sham mice.

Histograms summarize the c-Fos immunolabeled cell density comparison in deferent forebrain regions of SNI versus Sham mice including anterior ACC (A) posterior ACC (B) medial prefrontal cortex (C) and secondary motor cortex (D). SNI group, n=4; Sham group, n=4. A t-test demonstrated higher density of c-Fos-immunolabeled cells in cg2 of anterior ACC in SNI than that of Sham mice (A). E and F, left panels: representative images illustrate c-Fos immunolabeled cells in the aACC of the mouse from Sham (E) and SNI (F) groups. Red rectangle areas are amplified in right panels, respectively. Scale bars are 200  $\mu$ m in left panels and 50  $\mu$ m in right panels. Error bars represent S.E.M. Asterisk denotes significant difference between SNI and Sham groups. \*p<0.05.

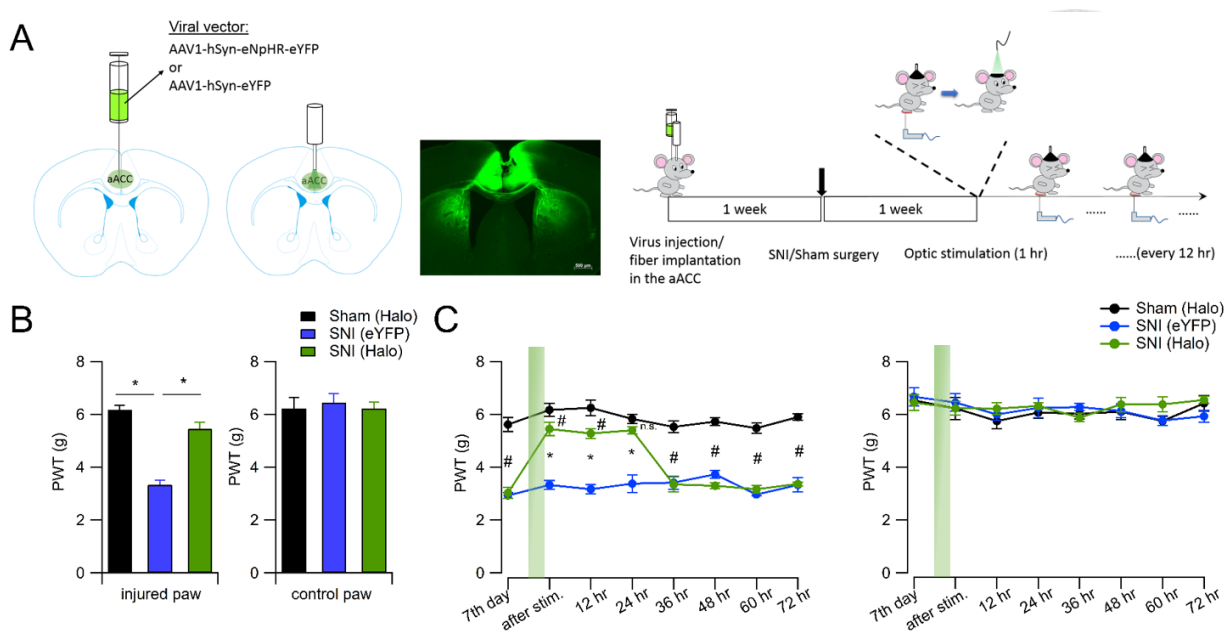


Figure 2. Causal examination of 1-hour photoinhibition in the aACC induced pain-relief in mechanical allodynia for at least 24 hours.

A, Schematics represent bilaterally injection of AAV encoded Halorhodopsin or eYFP as control and fiber implantation in the midline in the aACC for optogenetic manipulation (left panel). The representative picture shows Halo expression specifically in the aACC and fiber track (middle panel). Scale bars is 500  $\mu$ m. The right panel demonstrates the experimental design timeline. B, Histograms summarize the average paw withdrawal threshold (PWT) measured by von Frey test after 1-hour photoinhibition in the aACC. The left histogram shows average PWTs in the injured hind paw, and the right histogram is served as control data collected from contralateral non-injured hind paws. The experiment includes SNI Halo (green), SNI eYFP (blue) and Sham Halo (black) groups. One-way ANOVA followed by Bonferroni post hoc test demonstrated one-hour photoinhibition in the aACC significantly increased PWT in SNI mice right after the light stimulation. [SNI(eYFP) group,  $3.33 \pm 0.16$  g,  $n=6$ ; SNI(Halo) group,  $5.45 \pm 0.23$  g,  $n=6$ ; Sham(Halo) group,  $6.17 \pm 0.22$  g,  $n=6$ ;  $F=53.34$ ,  $p<0.0001$ ]. C, The plots summarize the PWT change in various time points after 1-hour green light stimulation (green shadow) in the aACC. The left plot summarizes PWTs collected from injured hind paw, and the right panel summarizes contralateral non-injured paws as control. The experimental design includes SNI Halo (green), SNI eYFP (blue) and Sham Halo (black) groups. A two-way ANOVA with repeated measures (groups x time factor) demonstrated a significant main effect of groups ( $F_{(2, 15)}=262.3$ ,  $p<0.0001$ ) in von Frey measurements of injured paws. Error bars represent S.E.M. Asterisk denotes significant difference between eYFP and Halo groups of SNI mice. #

denotes significant difference between SNI and Sham groups of Halo mice by Bonferroni post hoc test. \* $p < 0.05$ , # $p < 0.05$ .



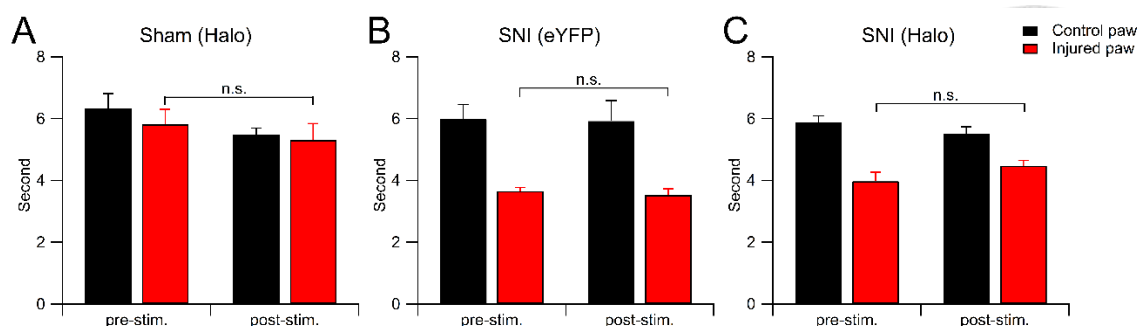


Figure 3. 1-hour photoinhibition in the aACC cannot alleviate thermal hyperalgesia induced by SNI.

A-C, Histograms summarize the average withdrawal response latency to infrared heat stimulation before and after 1-hour green light stimulation in the aACC (left two bars versus right two bars for each graph). The average latency of non-injured paws is shown in black bars, and injured paws are represented as red bars. A, Sham Halo group; B, SNI (eYFP) group; C, SNI (Halo) group. Repeat measurement t-tests demonstrated the latencies of the withdrawal responses in injured paws of SNI mice were not affected by one hour of green light stimulation in the aACC. [Sham (Halo), pre-stim= $5.813 \pm 0.4377$  s, post-stim= $5.313 \pm 0.4717$  s,  $n=5$ ,  $p>0.05$ ; SNI (eYFP), pre-stim= $3.65 \pm 0.1078$  s, post-stim= $3.533 \pm 0.1778$  s,  $n=6$ ,  $p>0.05$ ; SNI (Halo), pre-stim= $3.967 \pm 0.2831$  s, post-stim= $4.471 \pm 0.1695$  s,  $n=8$ ;  $p>0.05$ ]. Error bars represent S.E.M.

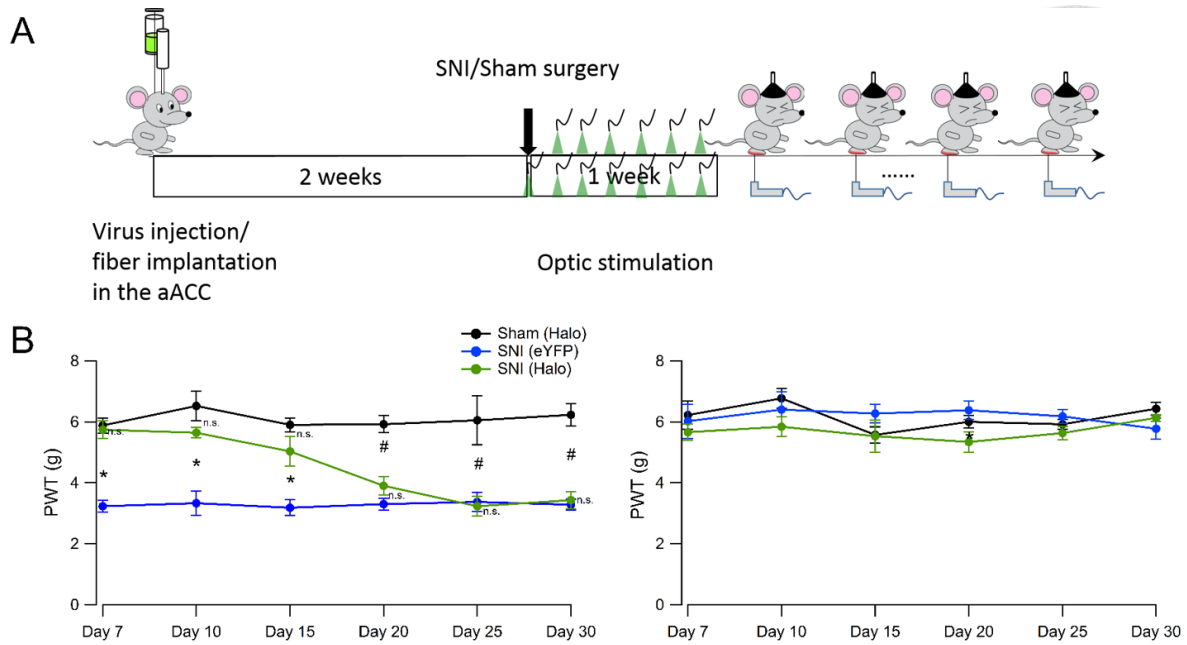


Figure 4. Repeated 1-hour photoinhibition in the aACC twice a day for a week can alleviate mechanical allodynia for at least one week since last light stimulation.

A, Schematic demonstrates the timeline of experimental procedure for 1-week repeated light stimulation. Various PWT measurements were performed after 1-week of 1-hour light stimulation twice a day protocol completion. B, Left and right panel shows the results of injured and non-injured hind paws average PWT, respectively. Various von Frey tests were performed among SNI eYFP (blue), SNI Halo (green) and Sham Halo (black) after the repeat light stimulation protocol. A two-way ANOVA (groups  $\times$  time factor) with repeated measures demonstrated a significant interaction ( $F(10, 80)=4.151$ ,  $p=0.0001$ ) and significant main effects of groups ( $F(2, 16)=158.1$ ,  $p<0.0001$ ) and time factor ( $F(5, 80)=3.958$ ,  $p=0.0029$ ) in injured paws. Error bars represent S.E.M. Asterisk denotes significant difference between eYFP and Halo groups of SNI mice. # denotes significant difference between SNI and Sham groups of Halo mice by Bonferroni post hoc test. \* $p<0.05$ , # $p<0.05$ .

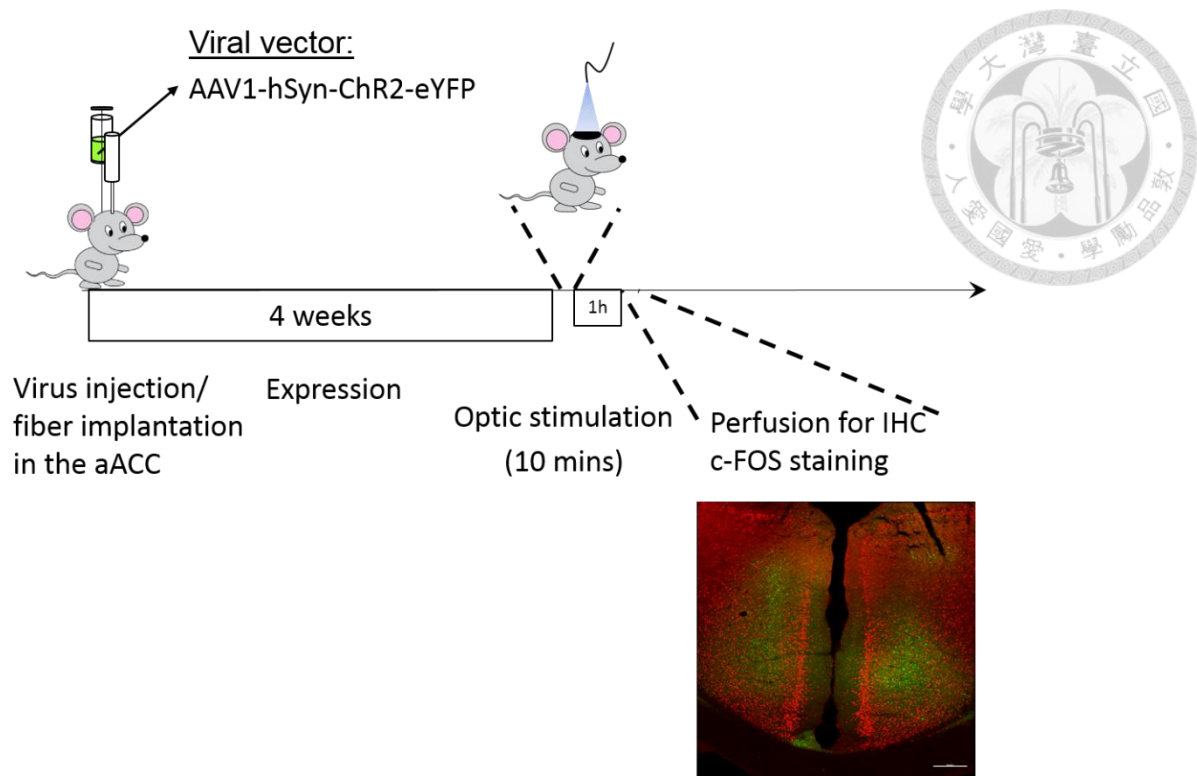


Figure 5. Schematic demonstrates experimental procedure for Table 1. The mice accepted 10 min of photoexcitation in the aACC for the preparation of c-Fos immunostaining of various brain regions. A representative picture of channelrhodopsin expression (green) and c-Fos positive cells (red) is shown below. Scale bar is 200  $\mu\text{m}$ .

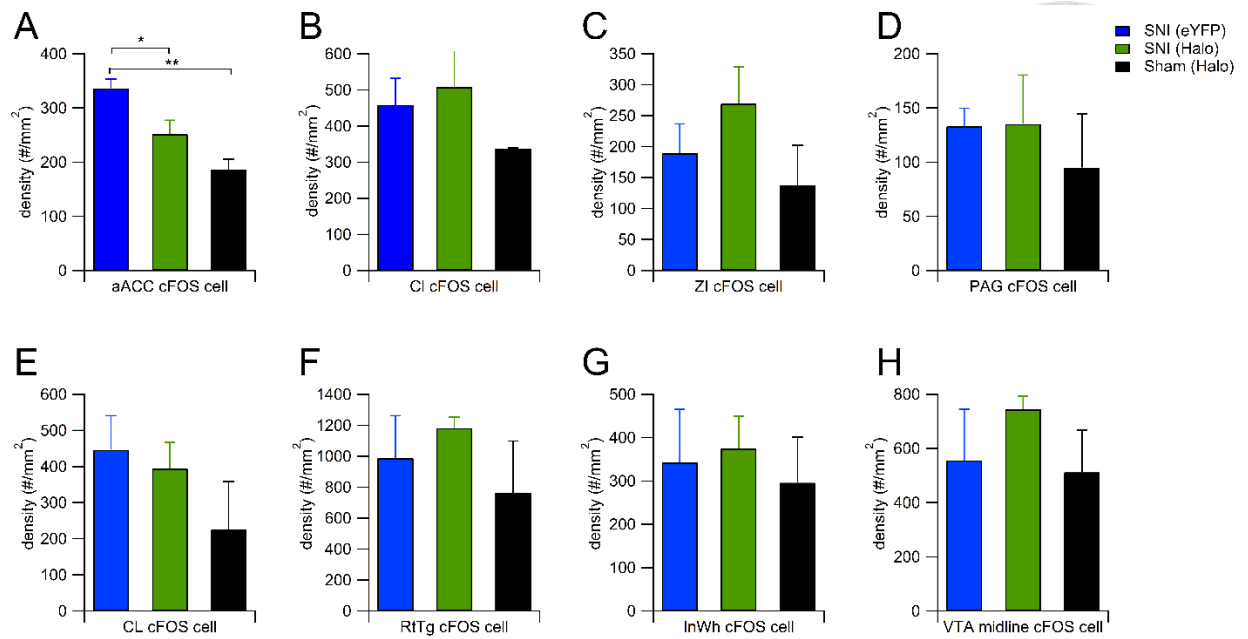


Figure 6. c-Fos immunolabelings after 1-hour aACC light stimulation in various selected brain regions.

A-H, Density of c-Fos-immunolabeled cells were compared among SNI eYFP (blue), SNI Halo (green) and Sham Halo (black) groups. The comparisons of different brain regions are shown in separated histograms from A-H. A, aACC; B, CL; C, ZI; D, DLPAG; E, CL; F, RtTg; G, InWh; H, VTA midline. Error bars represent S.E.M. Asterisk denotes significant difference between groups following one-way ANOVA with Bonferroni post hoc test. \*p<0.05, \*\*p<0.01.



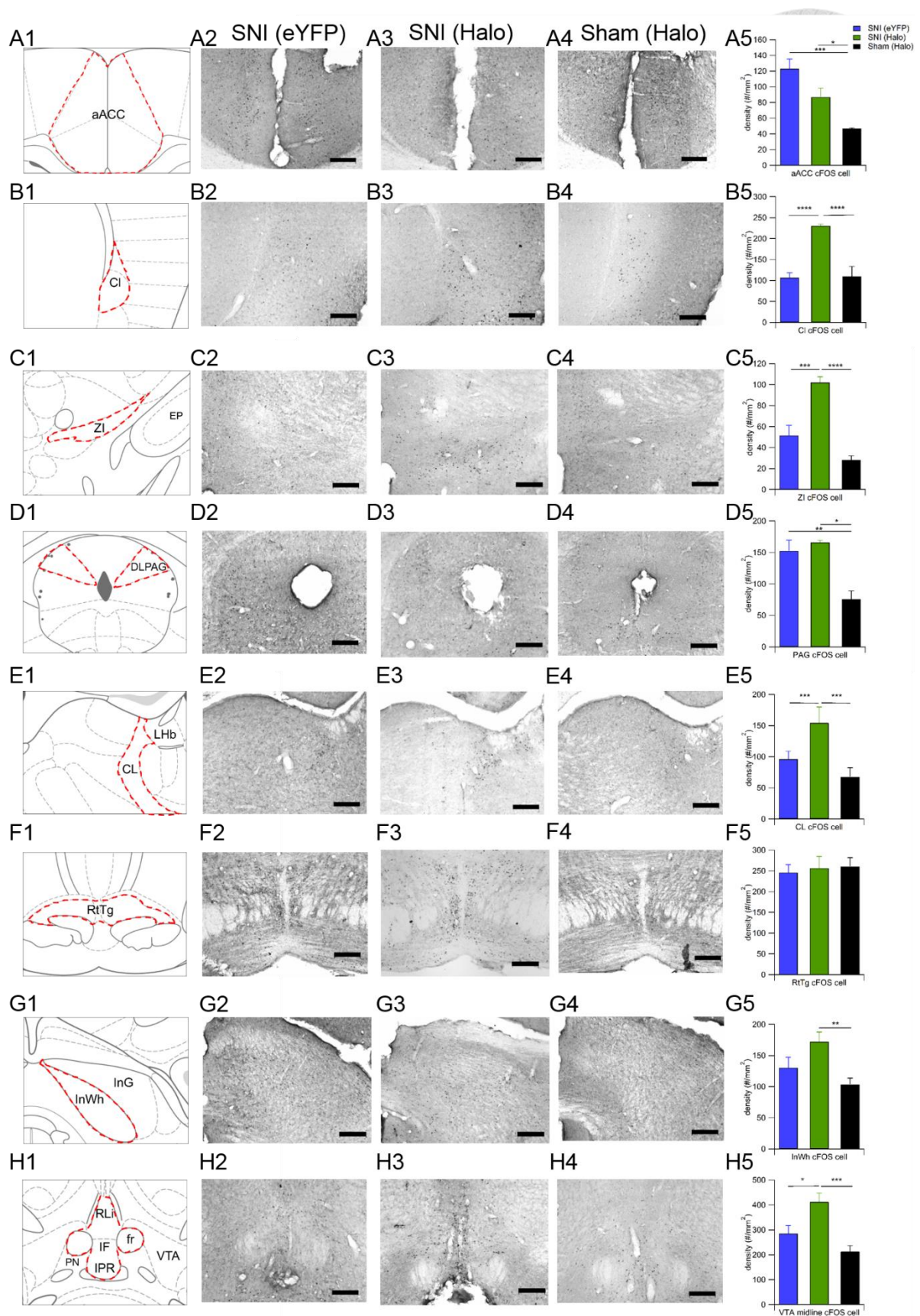


Figure 7. c-Fos immunolabelings after 1-week aACC light stimulations in various selected brain regions.

A1-H1, Red dashed line defines the selected region for c-Fos immunolabeling quantification in modified atlas from the mouse brain (Paxinos and Franklin, 2019). A1, aACC; B1, Cl; C1, ZI; D1, DLPAG; E1, CL; F1, RtTg; G1, InWh; H1, VTA midline.

Column 2-4 shows corresponding representative pictures of c-Fos immunolabeled cells among three groups of mice. Column 2, SNI mice with eYFP expression in the aACC, n=2. Column 3, SNI mice with Halo expression in the aACC, n=2. Column 4, Sham mice with Halo expression in the aACC, n=2. Scale bars are 200  $\mu$ m in all images panels.

A5-H5, Histograms summarize the average density of c-Fos immunolabeled cells in selective brain regions. Blue bars represent SNI eYFP groups, green bars represent SNI Halo groups and black bars represent Sham Halo groups. Error bars represent S.E.M. Asterisk denotes significant difference between groups following one-way ANOVA with Bonferroni post hoc test. \* $p < 0.05$ , \*\* $p < 0.01$ , \*\*\* $p < 0.001$ , \*\*\*\* $p < 0.0001$ .

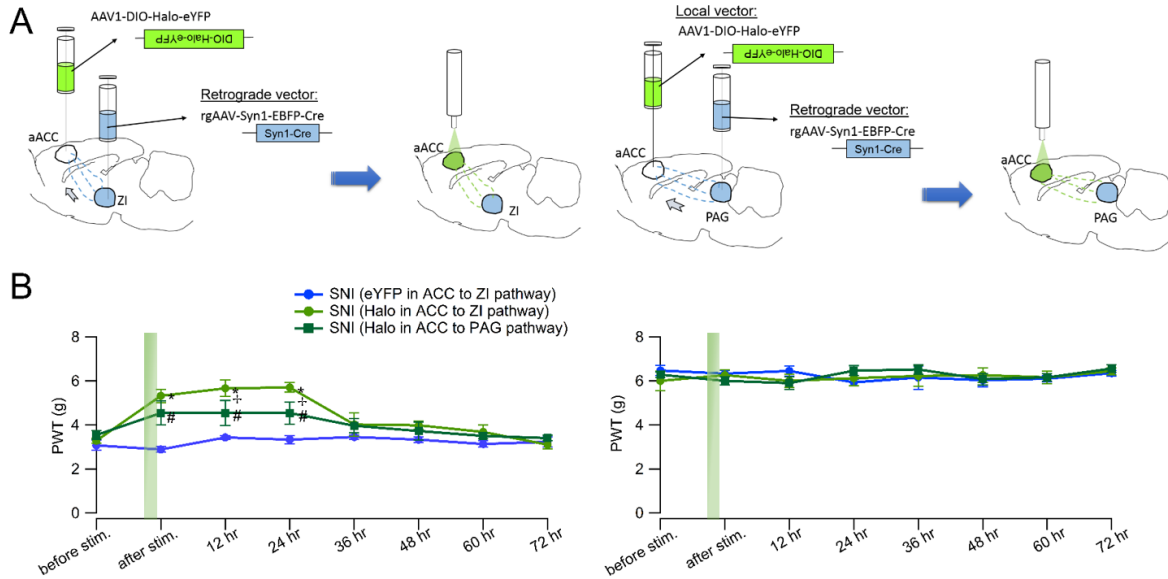


Figure 8. Causal examination of one-hour photoinhibition in selective ZI-projecting or PAG-projecting aACC neurons in alleviating mechanical allodynia.

A, Schematic representations of targeting ZI-projecting aACC neurons (left panel) and PAG-projecting aACC neurons (right panel) by using retrograde Cre-virus combining with DIO-Halorhodopsin. B, Plots summarize average PWTs change in injured (left panel) or non-injured (right panel) hind paws of SNI mice before and after 1-hour green light stimulation. Green shadows denote time point of light stimulation. Blue line chart represents SNI with eYFP expression in aACC-to-ZI efferents, light green line chart represents SNI with Halo expression in aACC-to-ZI efferents and deep green square line chart represents SNI with Halo expression in aACC-to-PAG efferents. A two-way ANOVA (groups  $\times$  time factor) with repeated measures demonstrated a significant interaction ( $F(14, 91)=5.58$ ,  $p<0.0001$ ) and significant main effects of groups ( $F(2, 13)=16.91$ ,  $p=0.0002$ ) and time factor ( $F(7, 91)=16.03$ ,  $p<0.0001$ ) in injured hind paws (left panel). Error bars represent S.E.M. Asterisk denotes significant difference between eYFP and Halo groups of SNI ZI-projecting mice. # denotes significant difference between eYFP ZI-projecting and Halo PAG-projecting groups of SNI mice. + denotes significant difference between ZI-projecting and PAG-projecting groups of SNI (Halo) mice with Bonferroni post hoc test. \* $p<0.05$ , # $p<0.05$ , +  $p<0.05$

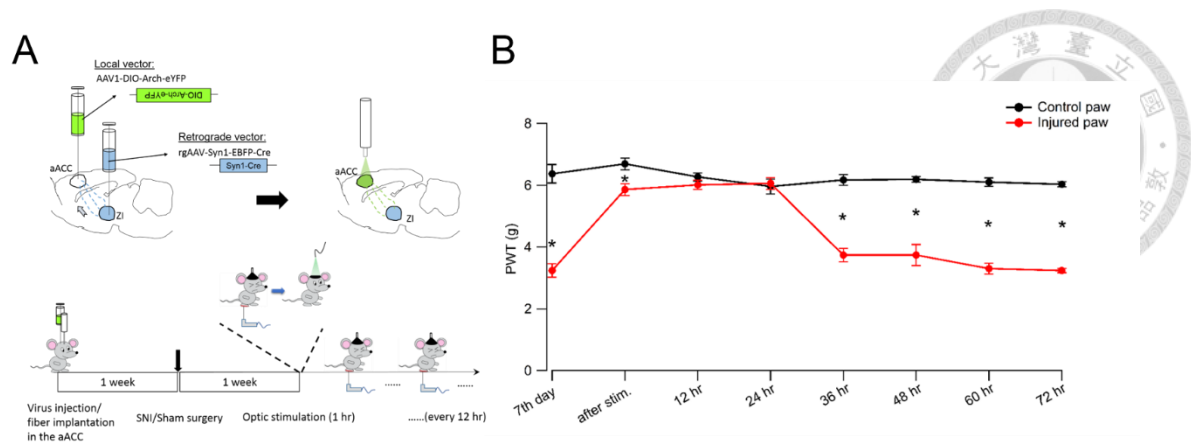


Figure 9. Control experiment of using alternative photoinhibition tool, Arch, to address the homeostasis issue caused by Halorhodopsin.

A, Schematic demonstrates retrograde targeting of ZI projecting aACC neurons by DIO-Arch combining with retro-Cre virus (top panel). Timeline graph demonstrates experimental procedure of one-hour photoinhibition in aACC-to-ZI efferents (bottom panel). Various von Frey tests were performed before and after one-hour photoinhibition in the ZI-projecting aACC neurons of SNI mice. B, Average PWTs of injured (red) and non-injured (black) hind paws of SNI mice at various time points before and after one-hour photoinhibition in aACC-to-ZI efferents. A two-way ANOVA (groups  $\times$  time factor) with repeated measures demonstrated a significant interaction ( $F(7, 84)=20.86$ ,  $p<0.0001$ ) and significant main effects of groups ( $F(1, 12)=552$ ,  $p<0.0001$ ) and time factor ( $F(7, 84)=24.92$ ,  $p<0.0001$ ). Error bars represent S.E.M. Asterisk denotes significant difference between injured and non-injured paws of SNI mice with Bonferroni post hoc test.  $*p<0.05$ .

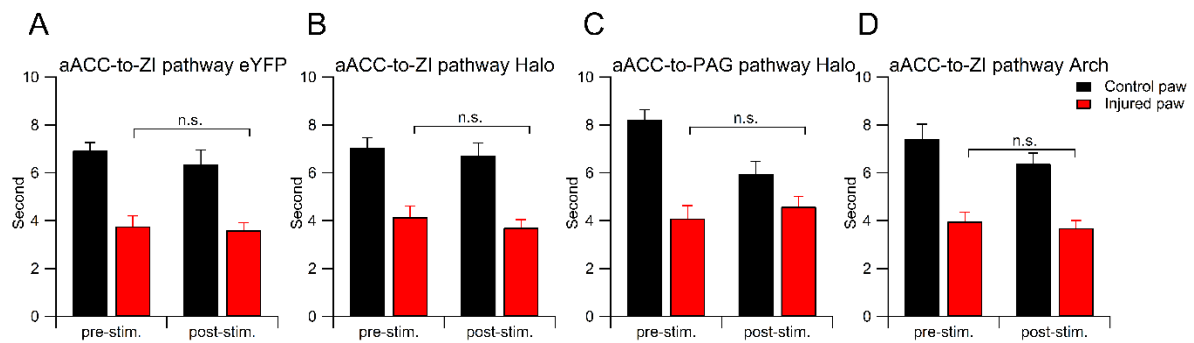


Figure 10. Thermal hyperalgesia induced by SNI were not affected by one-hour photoinhibition in selective aACC efferents.

A-D Histograms summarize the average withdrawal response latency to infrared heat stimulation on the injured (red bars) and non-injured (black bars) hind paws of SNI mice before and after one-hour green light stimulation in selective aACC efferents. For each bar graphs, left two bars represent pre-stimulation average latencies and right two bars represent post-stimulation average latencies. (B) and (D) bar graphs show photoinhibition in the ZI-projecting aACC neurons with Halo and Arch, respectively. (C) bar graph shows photoinhibition in the PAG-projecting aACC neurons with Halo. (A) bar graph is served as non-specific light-elicited effect control group with eYFP labeling of ZI-projecting aACC neurons. Repeat measurement t-tests demonstrated the latencies of the withdrawal responses in injured paws of SNI mice were not affected by one-hour green light stimulation. [aACC-to-ZI (eYFP), pre-stim= $3.755 \pm 0.4024$  s, post-stim= $3.605 \pm 0.281$  s,  $n=6$ ,  $p>0.05$ ; aACC-to-ZI (Halo), pre-stim= $4.145 \pm 0.4259$  s, post-stim= $3.705 \pm 0.3054$ ,  $n=6$ ,  $p>0.05$ ; aACC-to-PAG (Halo), pre-stim= $4.085 \pm 0.4718$  s, post-stim= $3.605 \pm 0.281$  s,  $n=4$ ;  $p>0.05$ ; aACC-to-ZI (Arch), pre-stim= $3.972 \pm 0.3475$  s, post-stim= $3.69 \pm 0.2885$  s,  $n=6$ ;  $p>0.05$ ]. Error bars represent S.E.M.

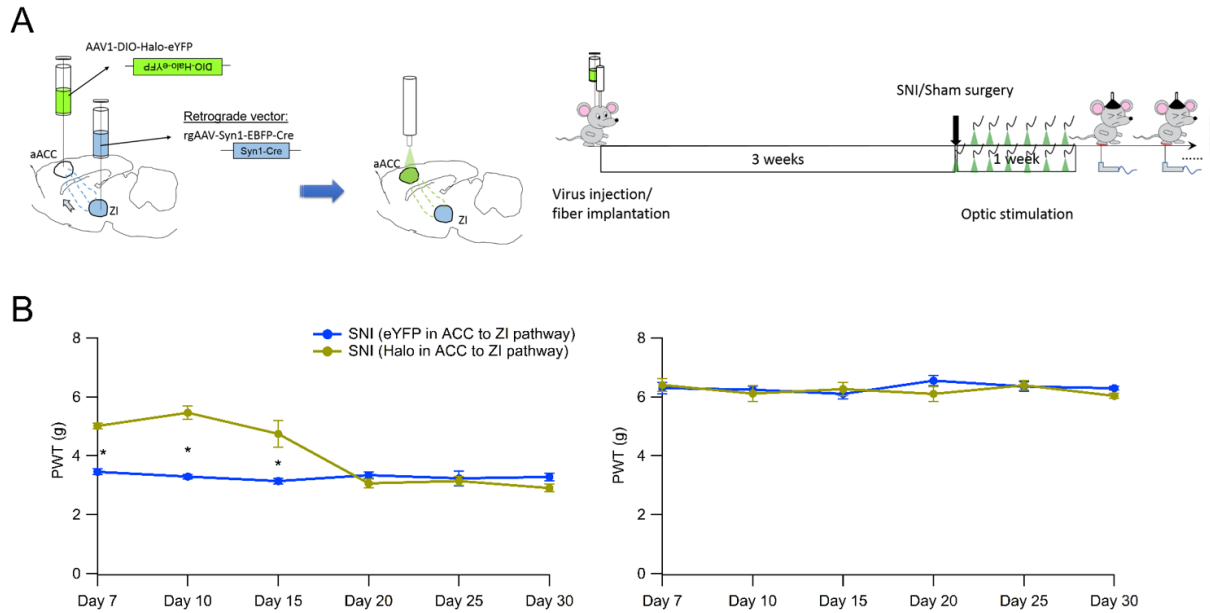


Figure 11. Repeated photoinhibition in ZI-projecting aACC neurons of SNI mice alleviates mechanical allodynia for more than a week since last light stimulation.

A, Schematic demonstrates retrograde targeting of ZI-projecting aACC neurons with DIO-halo and retro-Cre virus (left panel). Timeline graph shows experimental procedure for repeated light stimulation protocol after three weeks of viral expression and SNI surgery (right panel). B, Plots summarize the PWTs change of injured (left panel) and non-injured (right panel) hind paws of SNI mice. Various von Frey test were performed after the completion of repeated light stimulation protocol at different time points. Green line chart represents SNI with Halo expression in aACC-to-ZI pathway and Blue line chart represents SNI with eYFP expression in aACC-to-ZI pathway. A two-way ANOVA (groups  $\times$  time factor) with repeated measures demonstrated a significant interaction ( $F(5, 65)=21.22$ ,  $p<0.0001$ ) and significant main effects of groups ( $F(1, 13)=55.74$ ,  $p<0.0001$ ) and time factor ( $F(5, 65)=22.2$ ,  $p<0.0001$ ). Error bars represent S.E.M. Asterisk denotes significant difference between eYFP and Halo groups of SNI mice with Bonferroni post hoc test.  $*p<0.05$ .



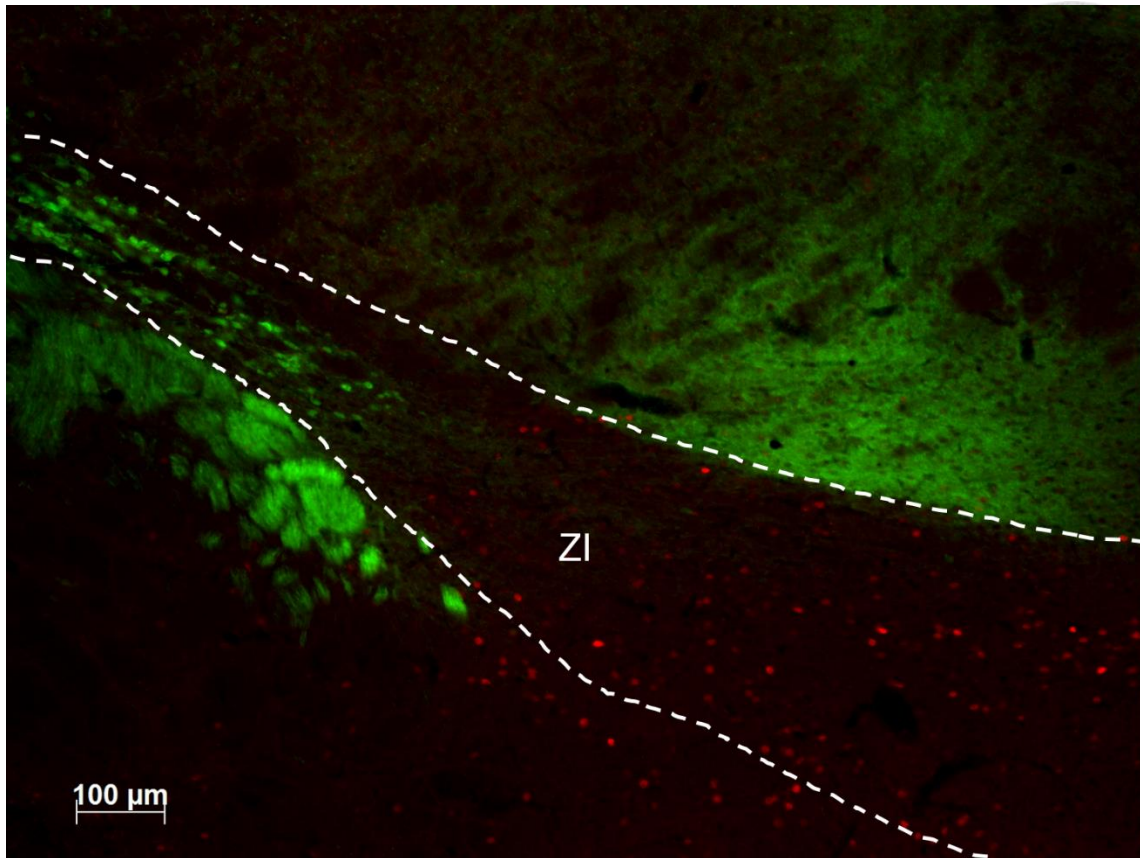


Figure 12. Image shows the c-Fos immunolabeled cells in the zona incerta of SN1 mouse recruited by one-hour photoinhibition in the aACC (red) and double-labeling with parvalbumin positive cells (green soma-like signals). The staining result shows no colocalization of these two populations.

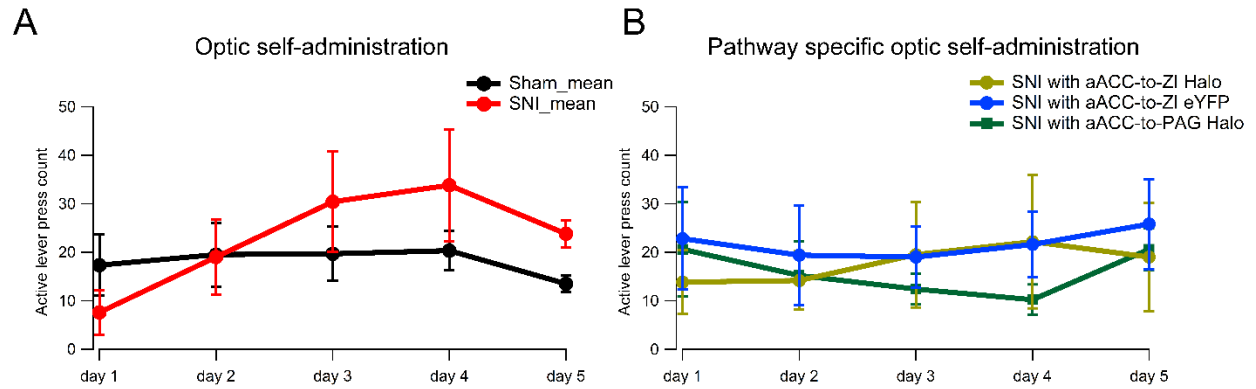


Figure 13. Employing optic self-administration paradigm to examine rewarding effect induced by photoinhibition in the aACC and selective aACC efferents.

A, Plot of average active lever pressing time across five sessions of optic self-administration in aACC Halo SNI (red) and Sham (black) mice. Every lever pressings trigger 5s of continuous green light stimulation in the aACC. A two-way ANOVA (groups  $\times$  sessions) revealed a significant interaction ( $F(4, 36)=2.828$ ,  $p=0.0388$ ) but not main effect of groups ( $F(1, 9)=0.5426$ ,  $p=0.4801$ ). B, Plot of average active lever pressing time across five sessions of optic self-administration in selective aACC efferents manipulation groups: aACC-to-ZI and aACC-to-PAG Halo SNI mice. The group of SNI mice with eYFP expression in ZI-projecting aACC neurons was served as control for green light stimulation. A two-way ANOVA (groups  $\times$  sessions) revealed neither interaction ( $F(8, 52)=0.8177$ ,  $p=0.59$ ) nor main effect of groups ( $F(2, 13)=0.1767$ ,  $p=0.84$ ).



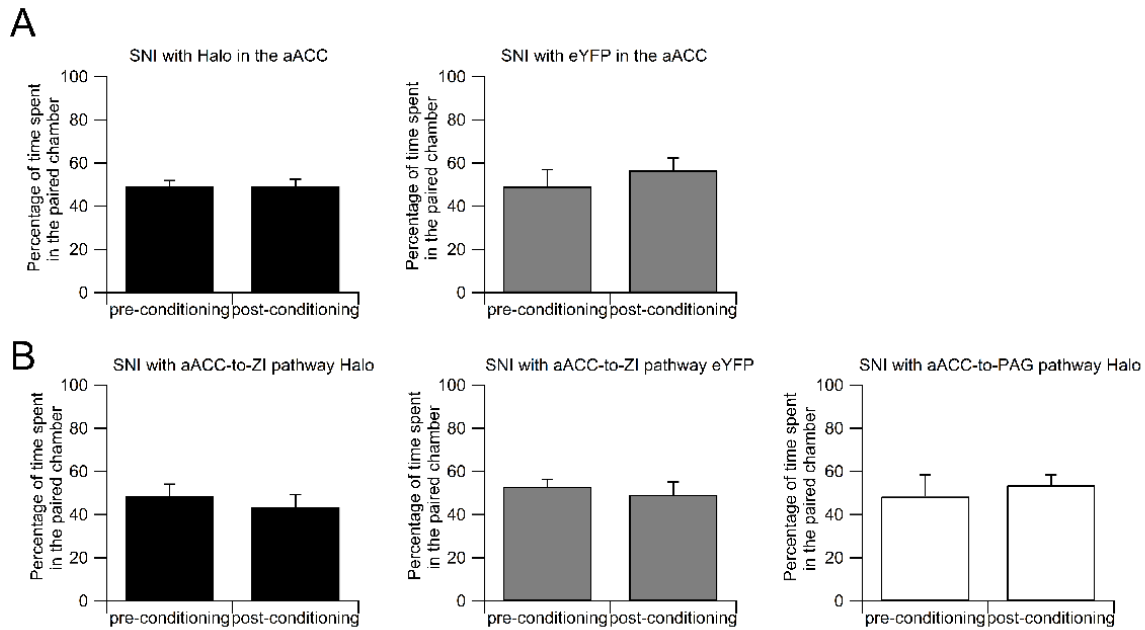


Figure 14. Conditioned place preference test was recruited to examine the potential reward resulting from pain-relief effect induced by one-hour photoinhibition in the aACC and selective aACC efferents of SNI mice.

A, Percentage of time spent in conditioned chamber before and after pairing with one-hour light stimulation in the aACC of SNI mice. Left histogram summarizes results from SNI Halo group and right histogram summarizes results from SNI eYFP group. Student t-tests revealed no significant preference over light stimulation-paired compartments in Halo group (A, left panel) of SNI mice [ $n = 11$  mice for SNI Halo,  $t = 0.01593$ , d.f. = 10,  $P = 0.9876$ ;  $n = 6$  mice for SNI eYFP  $t = 0.6382$ , d.f. = 5,  $P = 0.5514$ ].

B, Percentage of time spent in conditioned chamber before and after pairing with one-hour light stimulation in the selective aACC efferents of SNI mice. Left histogram summarizes result from aACC-to-ZI efferent Halo-expressing group, middle histogram summarizes result from aACC-to-ZI efferent eYFP-expressing group and right histogram summarizes result from aACC-to-PAG efferent Halo-expressing group. No significant preference over light-stimulation-paired chambers was observed in these three groups with repeated measures student t-test. [ $n = 8$  mice for SNI aACC-to-ZI Halo,  $t = 0.6527$ , d.f. = 7,  $P = 0.5348$ ;  $n = 8$  mice for aACC-to-ZI eYFP,  $t = 0.5257$ , d.f. = 7,  $P = 0.6154$ ;  $n = 5$  mice for aACC-to-PAG Halo,  $t = 0.8342$ , d.f. = 4,  $P = 0.4511$ ].

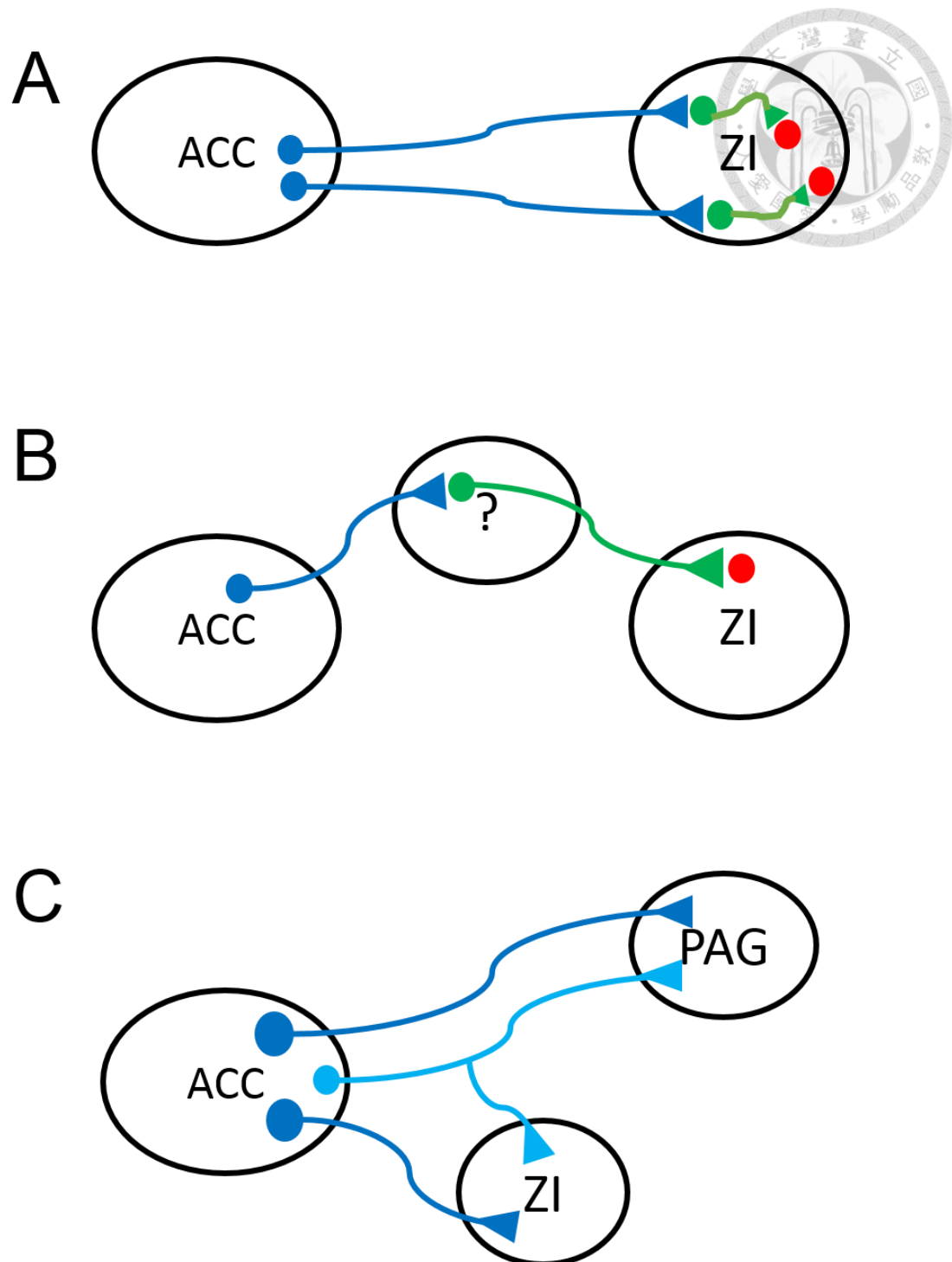
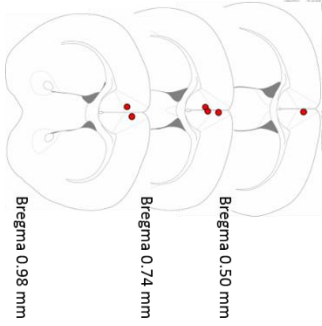


Figure 15. Schematic of aACC efferents involved in pain-relief.

A, ZI disinhibition (red cells) mediated by intra-ZI GABAergic interneurons (green).  
 B, ZI disinhibition mediated by an unidentified inhibitory brain region.  
 C, aACC sends respective excitatory efferent projections (blue) and axonal collaterals (light blue) to ZI and PAG.



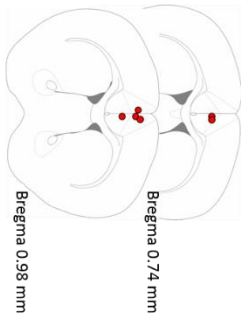
1-hour aACC SNI Halo



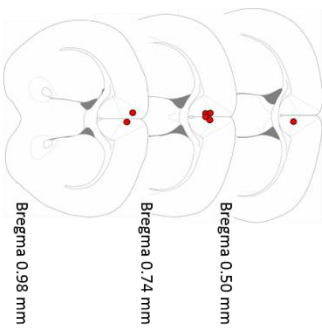
1-hour aACC SNI eYFP



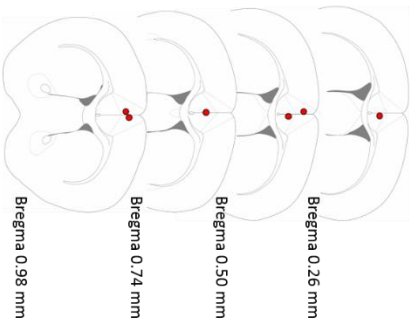
1-hour aACC Sham Halo



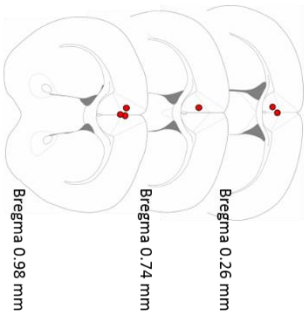
1-week aACC SNI Halo



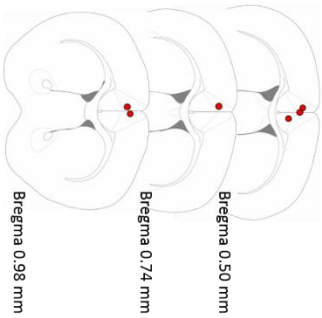
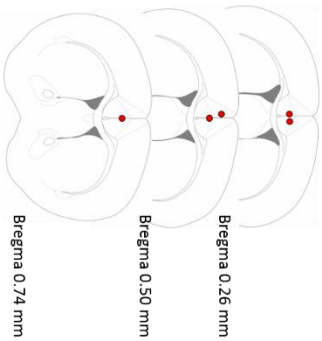
1-week aACC SNI eYFP

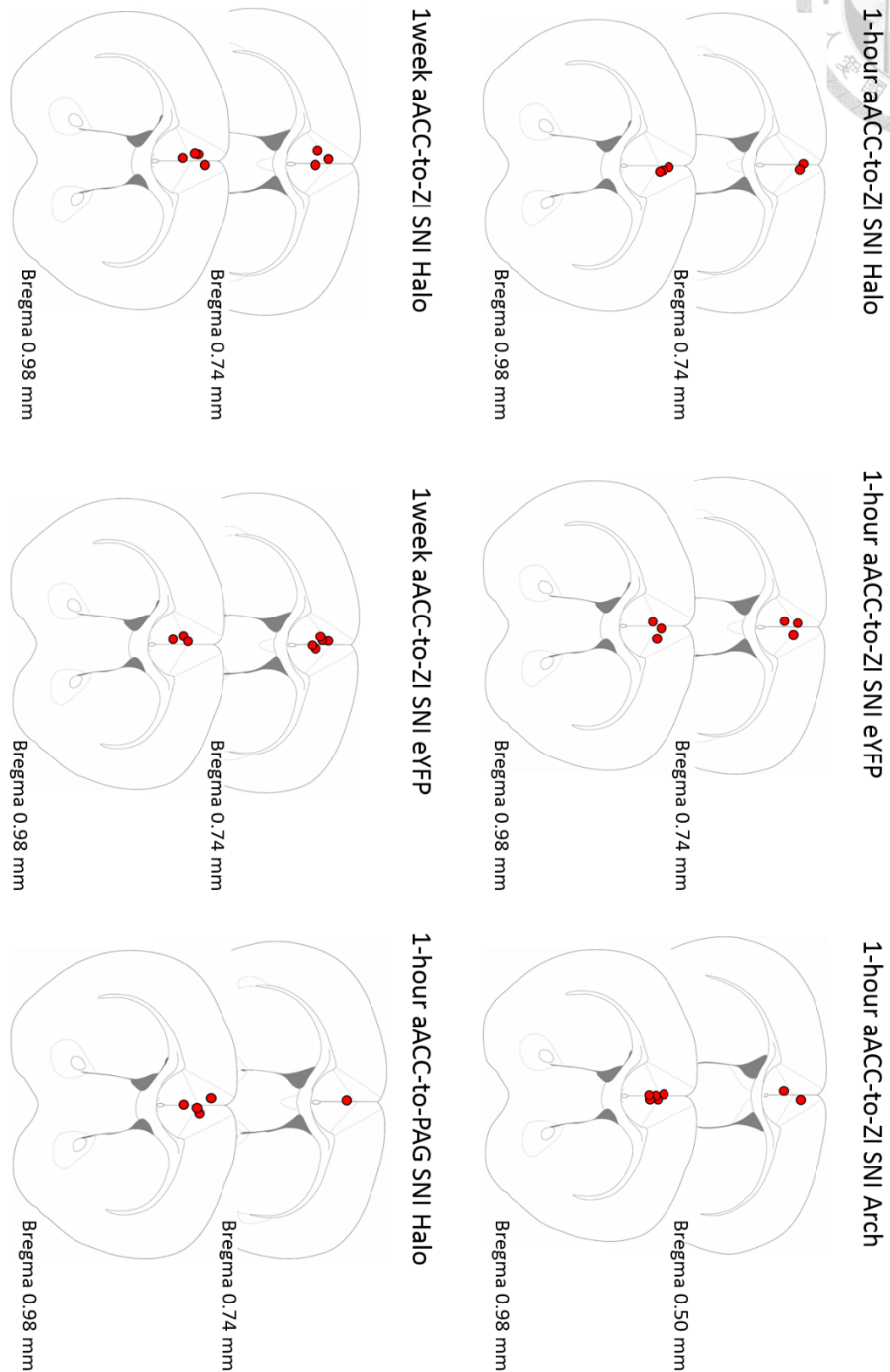


1-week aACC Sham Halo



Optic self-administration SNI Halo    Optic self-administration Sham Halo





Supplementary Figure. The terminal sites of fiber implantation were marked as red dot on the modified atlas (Paxinos and Franklin, 2019) for every mouse recruited in this study for behavioral experiments. Each graph corresponds to different groups of mice with label on top.